nature portfolio

https://doi.org/10.1038/s41565-021-01000-4

Supplementary information

Intercellular nanotubes mediate mitochondrial trafficking between cancer and immune cells

In the format provided by the authors and unedited

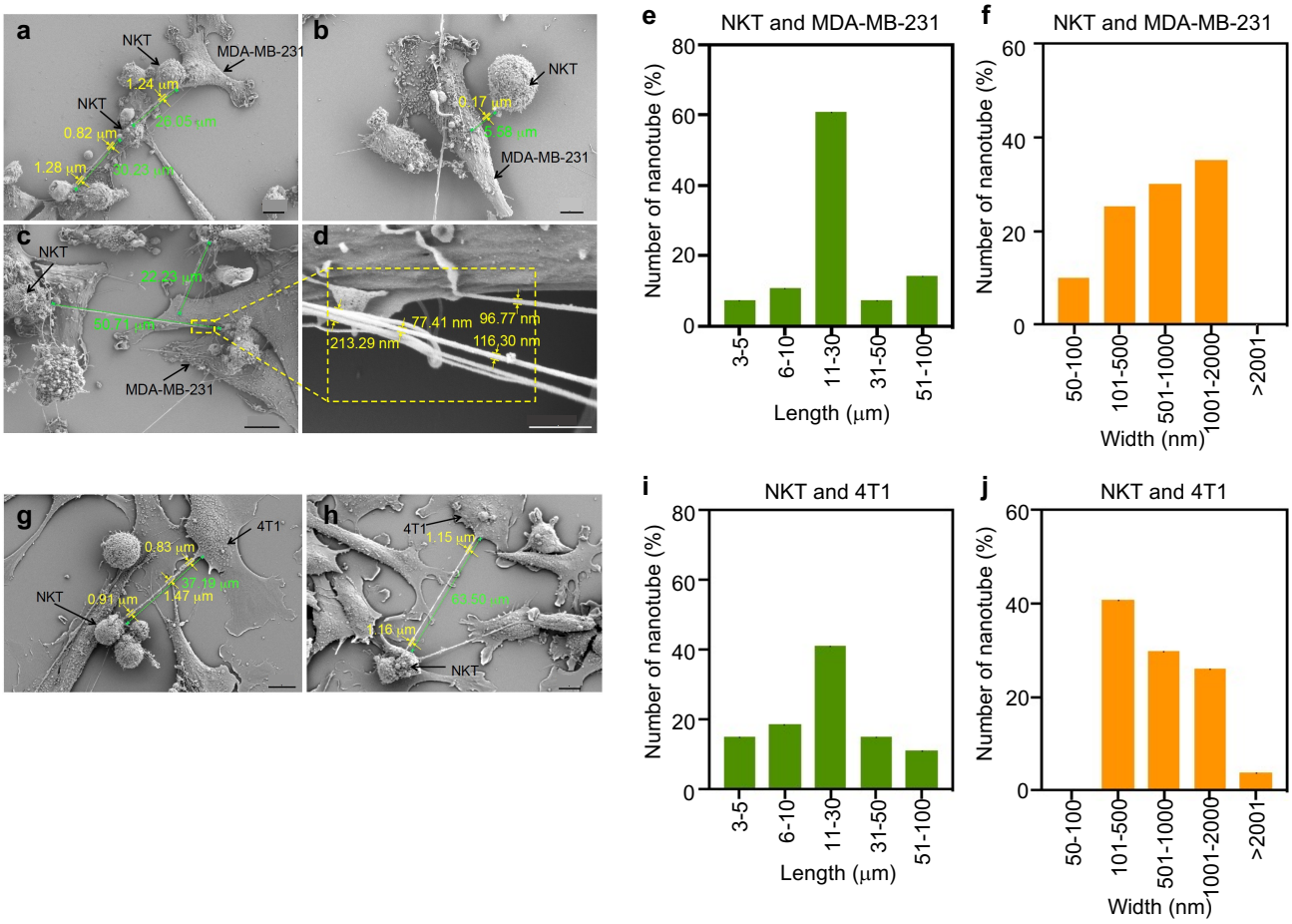

Supplementary Figure 1: Characterizing nanotubes between NKT cells and cancer cells. (**a**-**c**) Representative field emission scanning electron microscopy (FESEM) images showing nanotube connections between cancer cells (MDA-MB-231) and NKT cells (DN32.D3). The cells were cocultured in 1:1 mixture of respective cell media. The cells were fixed with gluteraldehyde after 16 h and imaged using FESEM. The length and the width are displayed on the respective images (scale bar a = 10 µm, b = 5 µm, c = 10 µm). (**d**) An aggregation of thin nanotubular structure can be observed in high magnification images (scale bar = 1µm). (**e**, **f**) Graphs show the distribution of the (**e**) length and (**f**) width of nanotubes. More than 15 images were used to calculate the length and width. (**g**) Representative FESEM images showing nanotube connections between cancer cells (4T1) and NKT cells (DN32.D3) (scale bar = 10 µm). (**h**) A representative image shows two cancer cells connecting to an immune cell *via* two nanotubes (scale bar = 10 µm). Graphs show the distribution of the (**i**) length and (**j**) width of nanotubes formed between the cancer and immune cells. (n > 15 images were used to calculate the length and width). All images were acquired under similar experimental condition.

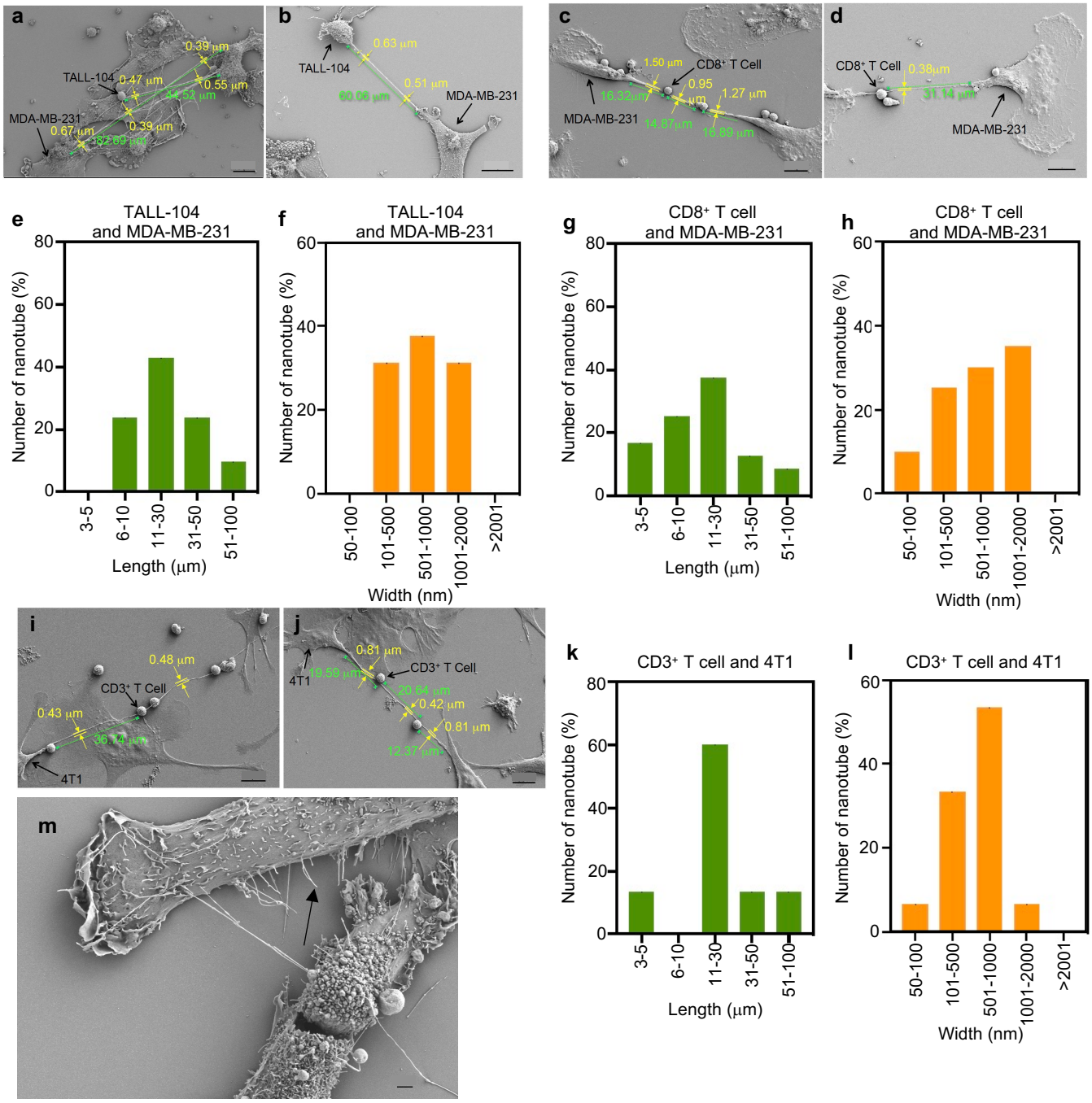

Supplementary Figure 2: Characterizing nanotubes between effector T cells and cancer cells. Representative FESEM images show nanotubes between human breast cancer cell MDA-MB-231 with (**a**, **b**) human T cell TALL-104 and (**c**, **d**) mouse CD8⁺ T cell. The cells were fixed after 16 h and imaged using FESEM. The length and the width are quantified on the respective images (scale bar a-d = 10 μm). In some cases, a network of nanotubes is visible (**a**). (**i, j**) Representative FESEM images showing nanotubes between mouse cancer cell (4T1) and mouse primary CD3⁺ T cells (scale bar i,j = 10 μm). (**e** – **h**, **k**, **l**) Graphs show the distribution of the length and width of nanotubes in the cancer-immune cells coculture. (n > 15 images were used to calculate the length and width). All images were acquired under similar experimental condition. (**m**) While number of nanotubes are formed, they do break during sample preparation. Black arrow shows broken ends (scale bar = 2μm).

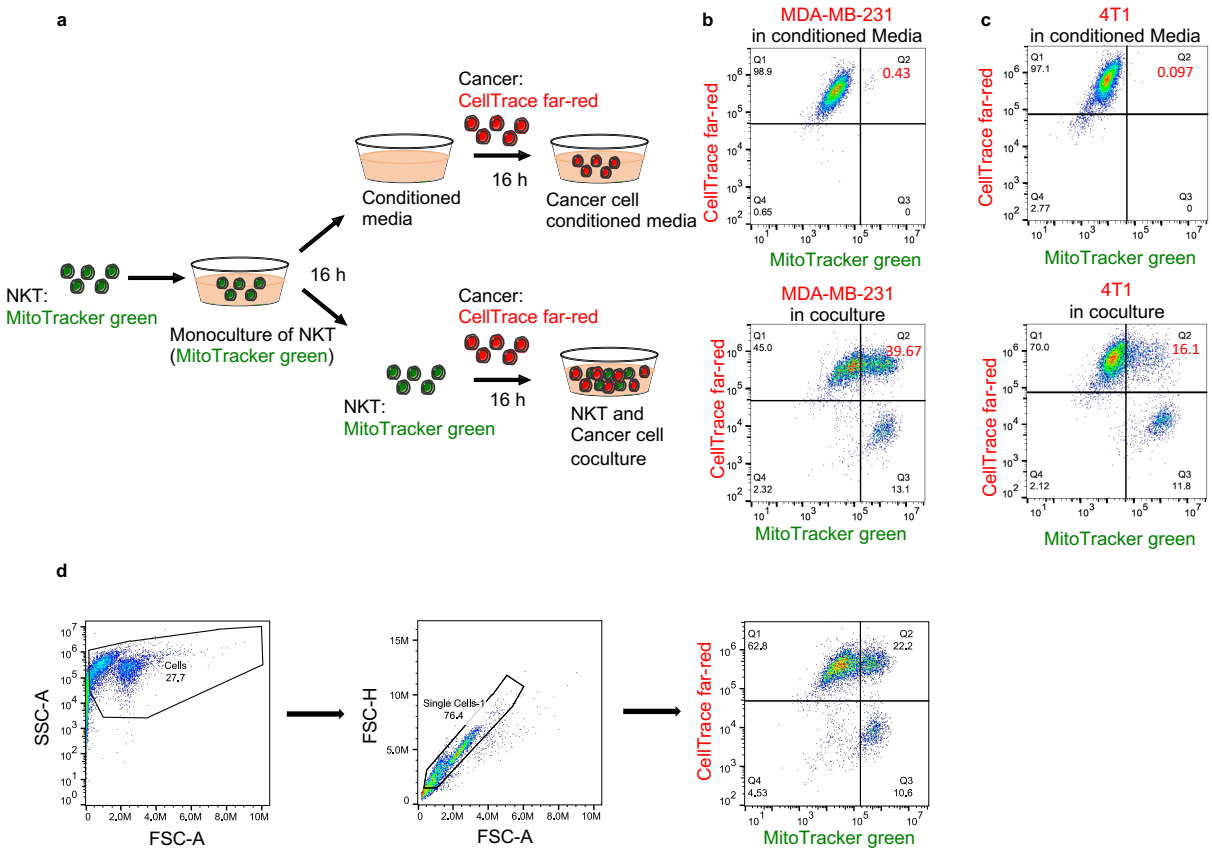

Supplementary Figure 3: Control study to test for MitoTracker green dye leakage from immune cells contributing to labeling of mitochondria of cancer cells. (**a**) Schematic representation of the conditioned media experiment. NKT cells were stained with MitoTracker green (0.5 μM), washed thoroughly as mentioned in the methods section, and cultured in complete media for 16 h. The conditioned media of NKT cells was collected and added to CellTrace far-red stained cancer cells for another 16 h. On the other hand, the MitoTracker stained NKT cells were cocultured with CellTrace far red stained cancer cells. Exact same amount of media has been used to avoid any dilution effect in the experiment. (**b**) Scatter plot showing absence of MitoTracker staining in the MDA-MB-231 cancer cells cultured in conditioned media of NKT cells (upper plot). The cancer cells cocultured with NKT cells showed transfer of mitochondria in MDA-MB-231 cells (lower plot). (**c**) Scatter plot showing absence of MitoTracker staining in the 4T1 cancer cells cultured in conditioned media of NKT cells (upper plot). The 4T1 cells cocultured with NKT cells showed transfer of mitochondria to 4T1 cells from NKT cells (lower plot). (**d**) Gating strategy for Flow cytometry analysis.

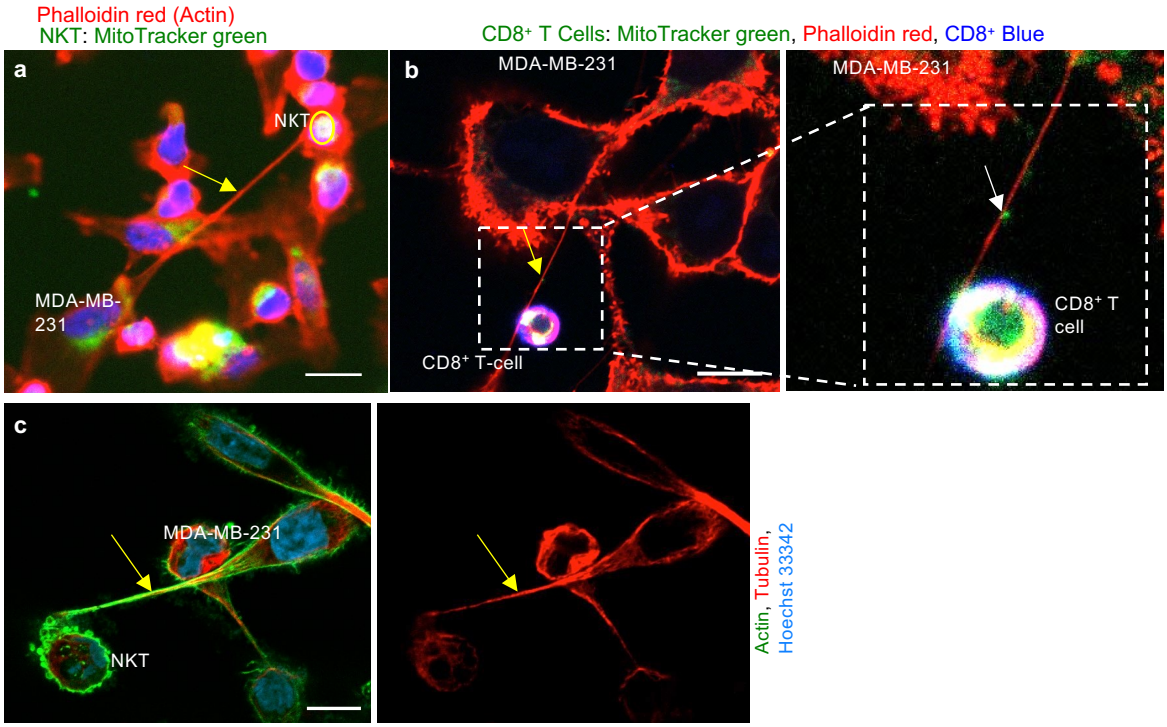

Supplementary Figure 4: (a) Representative images of cocultures of different immune and cancer cell types show the transfer of mitochondria *via* nanotubes made up of actin cytoskeletal elements. Immune cells were labeled first with MitoTracker green dye before coculture with cancer cells (unstained). The coculture was fixed after 16 h and stained with rhodamine phalloidin (red) to label the actin filaments in all cells. The combinations of immune and cancer cells are listed in the images and the images were acquired with either confocal or fluorescence microscope. The yellow arrow shows the nanotube between cancer and immune cell. The presence of the green signal in the cancer cell represents the transfer of the mitochondria from immune to cancer cell (scale bar = 20 μm). (**b**) Confocal image shows nanotube formation between a breast cancer cell (MDA-MB-231) and CD8⁺ T cell, and transfer of mitochondria from immune to cancer cell. Mitochondria of CD8⁺ T cells were labeled with MitoTracker green and employed in coculture assay with unstained MDA-MB-231 cells. After 16 h the coculture was fixed by 4% paraformaldehyde and immunostained with CD8⁺ antibody conjugated with BV-421 (blue) dye. The actin was stained with rhodamine phalloidin (red). The blue signal from the immune cell (CD8: BV-421) confirms the nanotube formation between cancer cell and CD8⁺ T cell. White arrow shows Mitotracker green in the nanotube (scale bar = 10 μm). (**c**) Representative confocal image showing presence of tubulin in the nanotube. MDA-MB-231 cells were cocultured with NKT cells for 16 h and immunolabeled with tubulin (red) antibody. Actin was stained with phalloidin green and nucleus was stained by Hoechst 33342. Single channel images are shown for clarity. Yellow arrows used to label nanotubes (scale bar = 10 μm).

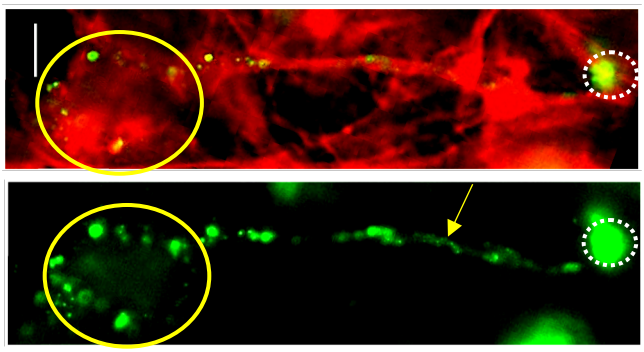

Supplementary Figure 5: Representative fluorescence microscopy image of coculture of $CD3^+$ T cells and 4T1 cells showing the nanotubes formed between cancer and immune cell. $CD3^+$ T cells were obtained from the splenocyte of $PhAM^{excised}$ (photo-activatable mitochondria) mice expressing a mitochondria-specific version of Dendra2. The Dendra2-labeled $CD3^+$ T cells were cocultured with unstained 4T1 cells. After 16 h, the coculture was fixed with paraformaldehyde and actin was stained with rhodamine phalloidin. The $CD3^+$ T cells were identified based on strong green signal and small size of the cell. The green fluorescence signal in the cancer cell is consistent with Dendra2-positive mitochondria being trafficked from immune cells to the cancer cells. Yellow arrows indicate the nanotube. Scale bar of 10 μm shown vertically.

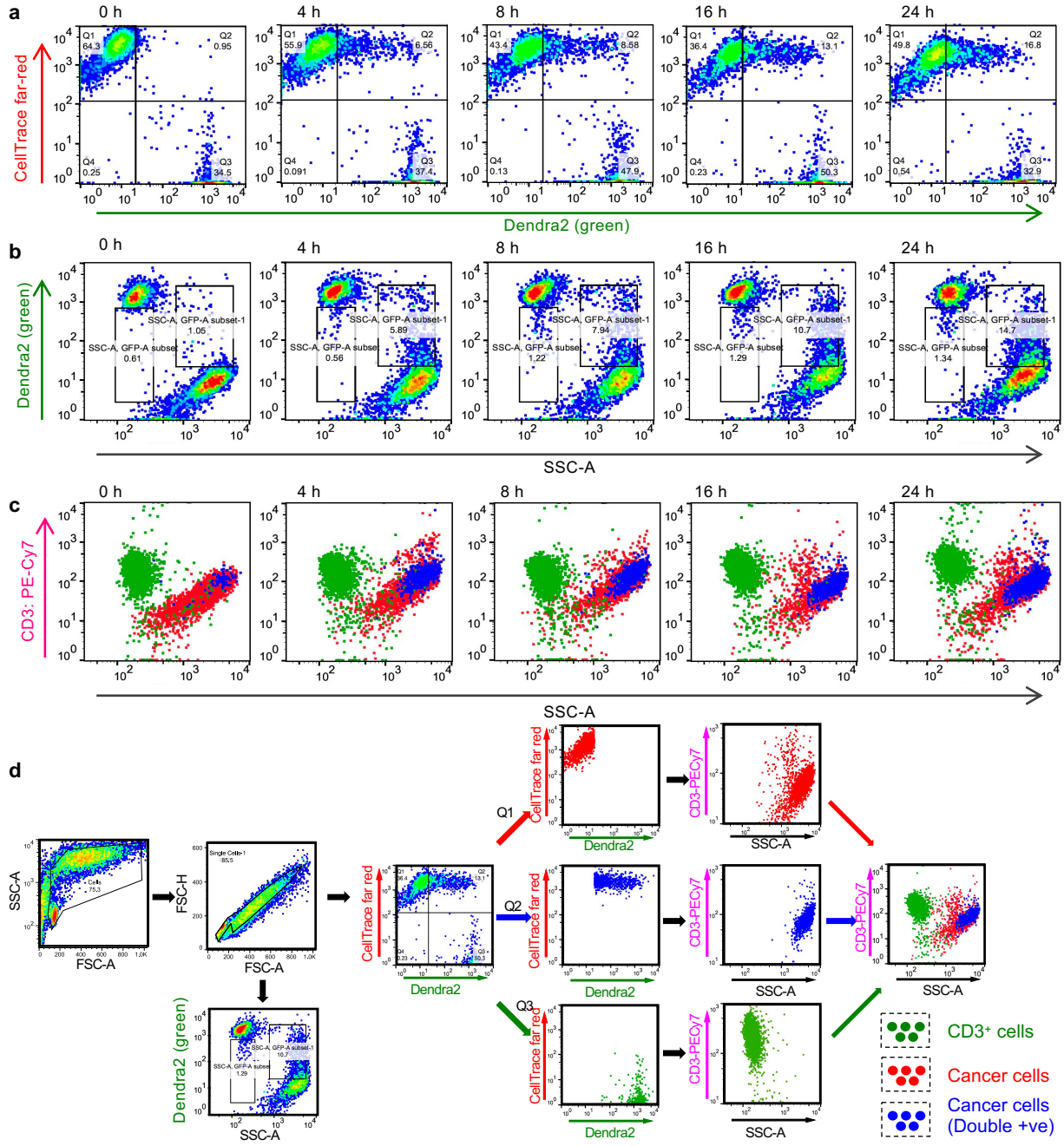

Supplementary Figure 6: Temporal and directional transfer of mitochondria between immune and cancer cells. (**a**) FACS plots show the transfer of mitochondria from CD3⁺ T cells to MDA-MB-231 cells over time. CD3⁺ T cells were obtained from the splenocyte of PhAM^{excised} mice expressing a mitochondria-specific version of Dendra2 monomeric fluorescent protein. The Dendra2-labeled CD3⁺ T cells were cocultured with CellTrace far-red stained MDA-MB-231 cells. The coculture was analyzed by flow cytometer at different time intervals. At 0 h the MDA-MB-231 cells (CellTrace far-red stained) and CD3⁺ T cells display as population corresponding to their fluorescent labeling in the scatter plot of flow cytometer analysis. With time, a new population representing both red and green (upper right quadrant) appears, consistent with the transfer of mitochondria from immune to cancer cells (directionality established elsewhere). (**b**) The plot represents the populations corresponding to CD3⁺ T cell and MDA-MB-231 cells at different levels of green intensity and side scattering. The smaller size of the CD3⁺ T cells than cancer cells make it easier to distinguish in terms of side scattering. The reduction of green intensity in a subpopulation of CD3⁺ T cells with a simultaneous increase in green intensity in MDA-MB-231 cells has been observed with time. (**c**) Representative plot of the coculture after staining with CD3 (PE-Cy7) specific antibody. The green population represents the dendra2 labeled CD3⁺ T cells (anti CD3-PECy7 stained) and the red population represents the CellTrace far-red stained cancer cells. The plot represents the population of cancer and immune cell depending on the fluorescence signal and size. The blue population indicates the cells having both red and green fluorescence. The blue population exactly superimposed with the population of the cancer cells and signifies the transport of the mitochondria from immune cells to cancer cells. (**d**) Figure shows the gating and analysis strategy, which validates that the transfer of Dendra2-positive mitochondria from immune to cancer cells.

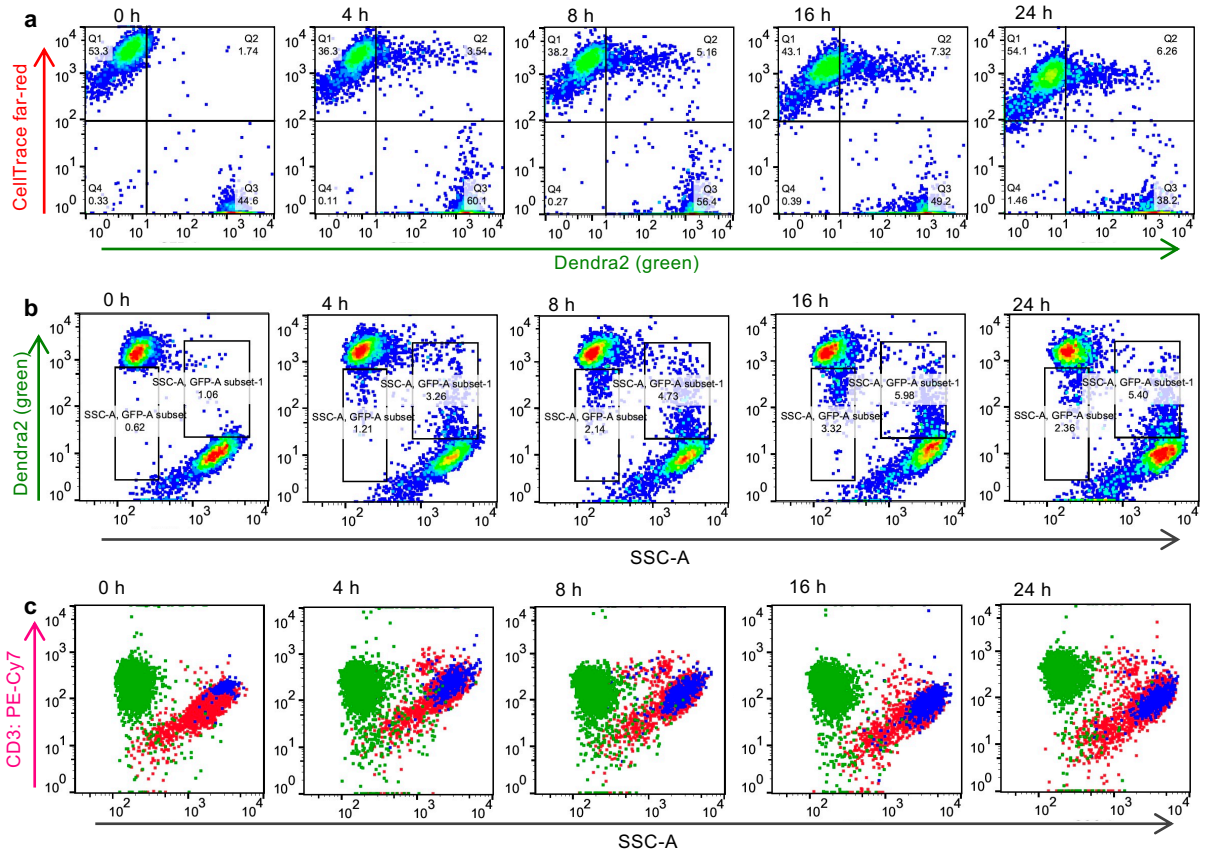

Supplementary Figure 7: Temporal and directional transfer of mitochondria between immune and cancer cells. (**a**) Time dependent transfer of mitochondria from CD3⁺ T cells to 4T1 cells. CD3⁺ T cells were obtained from the splenocyte of PhAM^{excised} mice expressing Dendra2 fluorescent protein in mitochondria. The Dendra2-labeled CD3⁺ T cells were cocultured with CellTrace far red stained 4T1 cells. The coculture was analyzed by flow cytometer at different time intervals. At 0 h the 4T1 cells (CellTrace far-red stained) and CD3⁺ T cells display as the populations corresponding to their fluorescent labeling in the scatter plot of flow cytometer analysis. With time, a new population representing both red and green (upper right quadrant) appears, consistent with the transfer of mitochondria from immune to cancer cells. (**b**) The plot represents the populations corresponding to CD3⁺ T cells to 4T1 cells at different green intensity and side scattering. The smaller size of the CD3⁺ T cells than cancer cells make it easier to distinguish in terms of side scattering. The reduction of green intensity in a subpopulation of CD3⁺ T cells with a simultaneous increase in green intensity in 4T1 cells has been observed with time. (**c**) Representative plot of the coculture after staining with CD3 (PE-Cy7) specific antibody. The green population represents the CD3⁺ T (anti CD3-PECy7 stained) cells and the red population represents the CellTrace far-red stained cancer cells. The plot represents the population of cancer and immune cell depending on the fluorescence signal and size. The blue population indicates the cells having both red and green fluorescence. The blue population exactly superimposed with the population of the cancer cells on side scatter (SSC) and signifies the transport of the mitochondria from immune cells to cancer cells. The similar gating strategy of Supplementary Fig 6d has been used.

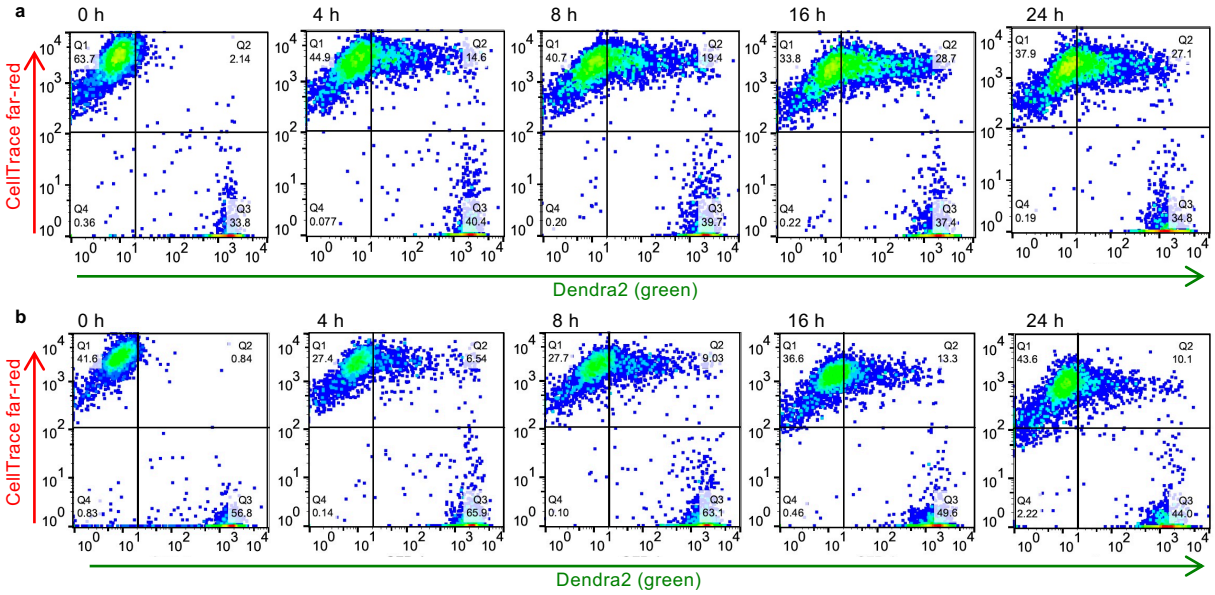

Supplementary Figure 8: (**a**) Time dependent transfer of mitochondria from CD8⁺ T cells to MDA-MB-231 cells. CD8⁺ T cells were obtained from the splenocyte of PhAM^{excised} mice. The Dendra2-labeled CD8⁺ T cells were cocultured with CellTrace far-red stained MDA-MB-231 cells. The coculture was analyzed by flow cytometer at different time intervals. At 0 h the MDA-MB-231 cells (CellTrace far-red stained) and CD8⁺ T cells display as distinct populations corresponding to their fluorescent labeling in the scatter plot of flow cytometer analysis. With time, a new population representing both red and green (upper right quadrant) appears, consistent with the transfer of mitochondria from immune to cancer cells. (**b**) Time dependent analysis of coculture of CD8⁺ T cells and 4T1 cells. The similar gating strategy of Supplementary Fig 6d has been used.

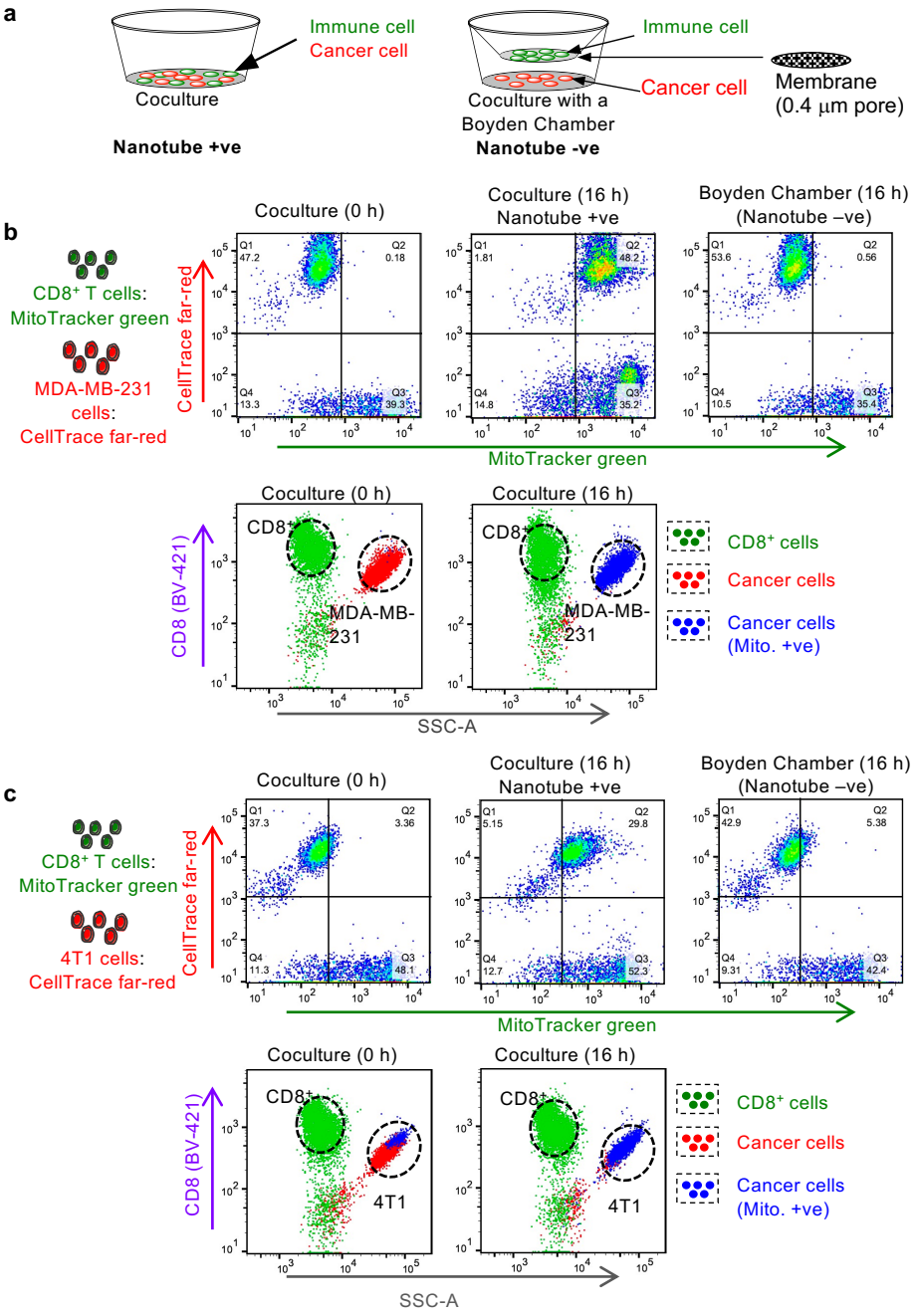

Supplementary Figure 9: (**a**) Schematic shows study design to quantify the transfer of mitochondria from immune cells to cancer cells over time. Cancer cells (MDA-MB-231 or 4T1) and CD8⁺ T cells were stained with CellTrace far-red and MitoTracker green respectively and added to the coculture. The coculture was analyzed by flow cytometer. CD8⁺ T cells were obtained from the splenocyte of BALB/c mice. (**b**) Scatter plot showing transfer of mitochondria from primary CD8⁺ T cells to MDA-MB-231 cells. At 0 h the cells exhibit as distinct populations according to their fluorescence signal. After 16 h a new population representing both red and green (upper right quadrant) appears, consistent with the transfer of mitochondria from immune to cancer cells. The coculture assay in presence of Boyden chamber shows negligible transfer of mitochondria. The second row represents the individual population of CD8⁺ T cells and MDA-MB-231 cells in SSC vs CD8 antibody scatter plot. The green population represents the CD8⁺ T (MitoTracker green and anti CD8-BV421 stained) cells and the red population represents the CellTrace far-red stained cancer cells. The plot represents the population of cancer and immune cell depending on the fluorescence signal and size. The blue population indicates the cells having both red and green fluorescence. The blue population exactly superimposed with the population of the cancer cells and signifies the transport of the mitochondria from immune cells to cancer cells. (**c**) Transfer of mitochondria from primary CD8⁺ T cells to 4T1 cells. Gating strategy has been discussed in Supple. Fig. 6d. Dendra2 was replaced with MitoTracker green and CD3 PE-Cy7 was replaced with CD8 BV-421.

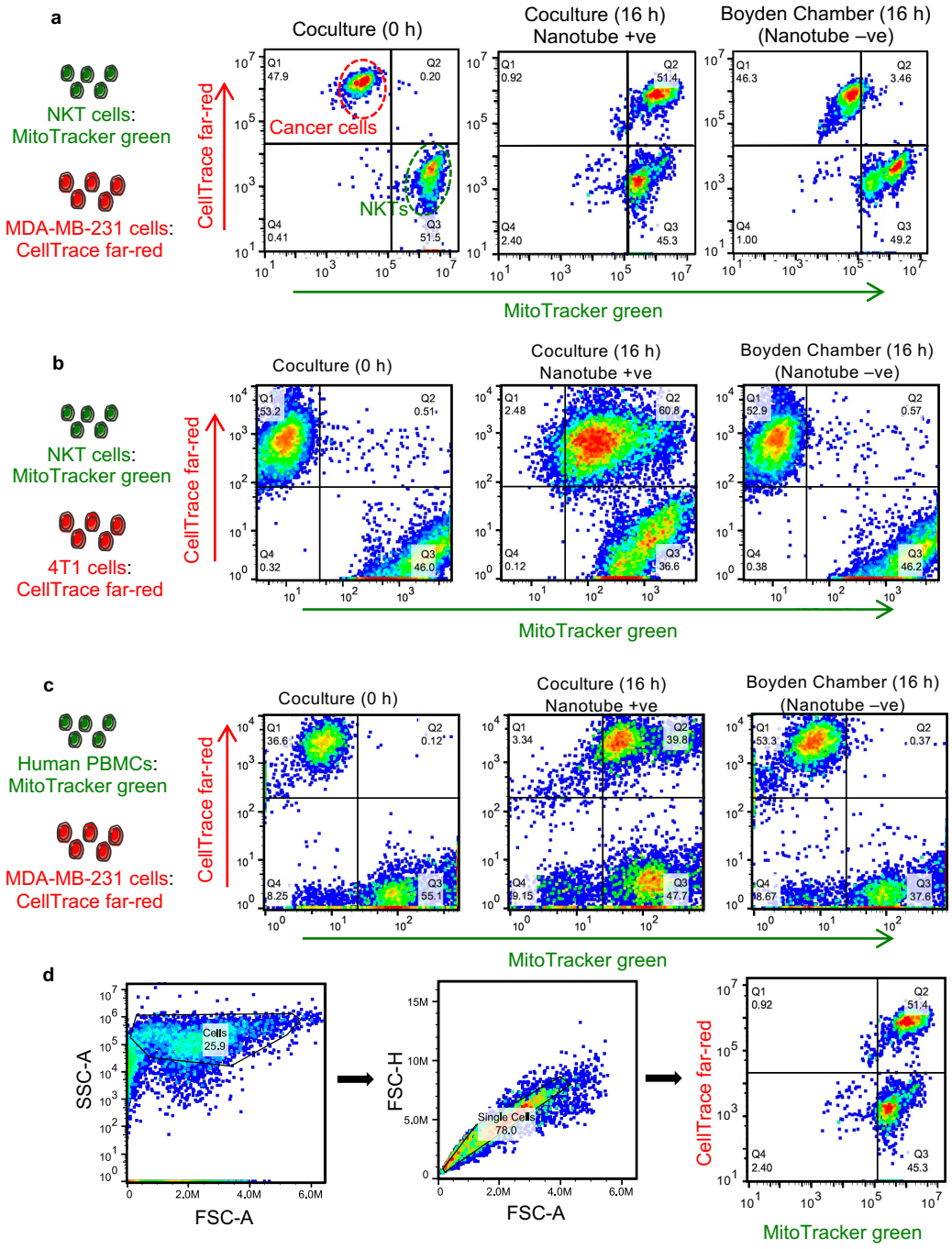

Supplementary Figure 10: (**a**) Transfer of mitochondria from NKT cells to MDA-MB-231 cells. The NKT cells and MDA-MB-231 cells were stained with MitoTracker green and CellTrace far-red respectively and employed in coculture assay. The coculture was analyzed by flow cytometer. FACS plots show at 0 h the cancer cells (CellTrace far-red stained) and NKT cells (MitoTracker green stained) display the population corresponding to their fluorescent labeling in the scatter plot of flow cytometer analysis. After 16 h a new population representing both red and green (upper right quadrant) appears, consistent with the transfer of mitochondria from immune to cancer cells. Similar experiment was also performed in a Boyden Chamber, which allows paracrine and exosomal transfer between the two cell types maintained in separate chambers but not nanotube connections. FACS plots show minimal transfer of mitochondria with time in the Boyden assay. (**b**) Transfer of mitochondria from NKT (DN32.D3) cells to 4T1 cells and (**c**) from human PBMCs to MDA-MB-231 cells under similar experimental condition. After 16 h a new population representing both red and green (upper right quadrant) appears, consistent with the transfer of mitochondria from PBMCs to cancer cells. The coculture assay in presence of Boyden Chamber shows minimal transfer of mitochondria. (**d**) Gating strategy for flow cytometric analysis.

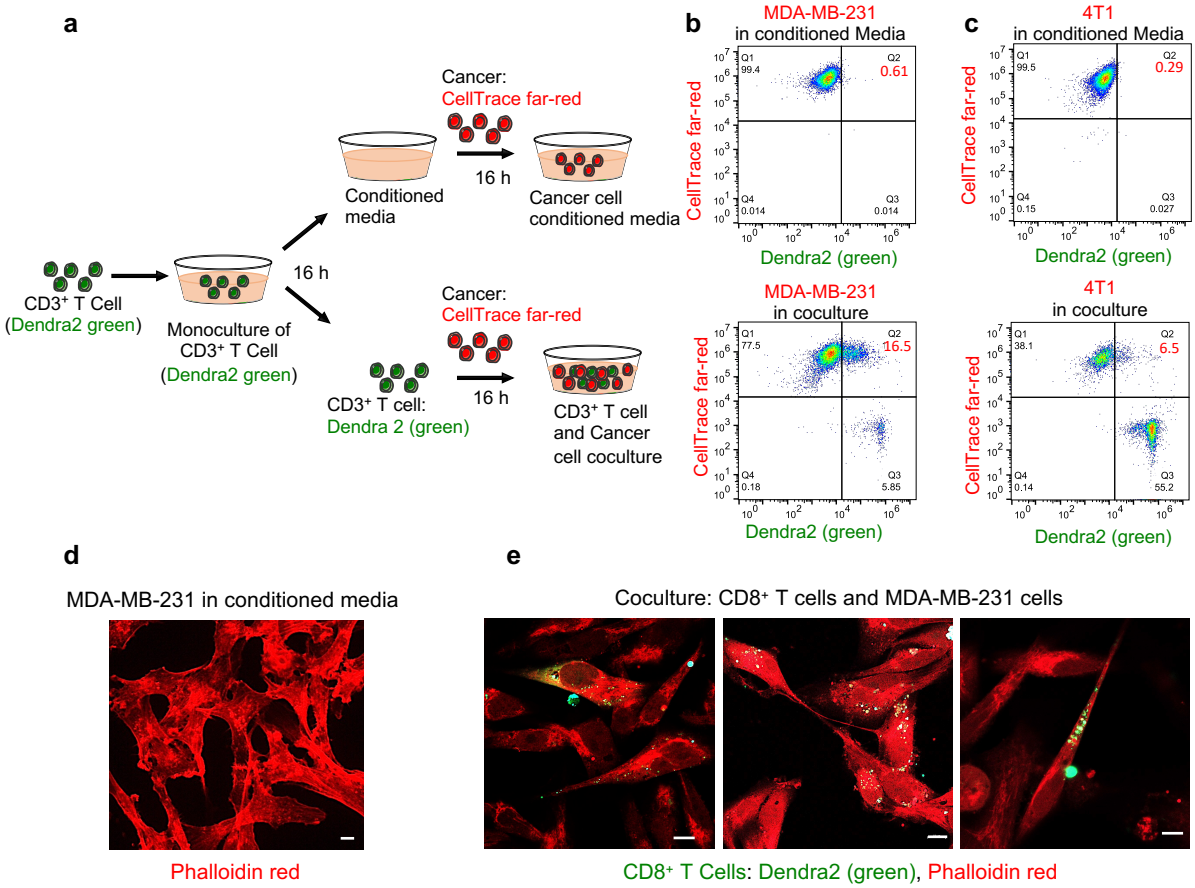

Supplementary Figure 11: Control study to test for Dendra2 leakage from immune cells contributing to labeling of cancer cells. (**a**) Schematic representation of the conditioned media experiment with Dendra2 CD3⁺ T cells and cancer cells (MDA-MB-231 and 4T1). CD3⁺ T cells were obtained from the splenocyte of PhAM^{excised} mice expressing Dendra2 fluorescent protein in mitochondria. CD3⁺ T cells were cultured in complete media for 16 h. The conditioned media of CD3⁺ T cells was collected and added to CellTrace far-red stained cancer cells for another 16 h. On the other hand, the Dendra2 labeled CD3⁺ T cells were cocultured with CellTrace far-red stained cancer cells in a separate experiment. Exact same amount of media has been used to avoid any dilution effect in the experiment. The similar gating strategy of Supplementary Fig 6d has been used. (**b**) Scatter plot showing absence of Dendra2 (green) staining in the MDA-MB-231 cancer cells cultured in conditioned media of CD3⁺ T cells (upper plot). The cancer cells cocultured with CD3⁺ T cells showed transfer of mitochondria (Dendra2-positive) in MDA-MB-231 cells (lower plot). (**c**) Scatter plot showing absence of Dendra2 (green) staining in the 4T1 cancer cells cultured in conditioned media of CD3⁺ T cells (upper plot). The 4T1 cells cocultured with CD3⁺ T cells showed transfer of mitochondria to 4T1 cells (lower plot). (**d**) Representative fluorescence microscopy image of MDA-MB-231 cells cultured in the conditioned media of Dendra2 labeled CD3⁺ T cells. Absence of green signal in the cancer cells signifies the absence of nonspecific leakage of Dendra2 labeled mitochondria from CD3⁺ T cells in cultured media. (**e**) Representative fluorescence microscopy image of MDA-MB-231 cells cocultured with Dendra2 labeled CD3⁺ T cells. Green signal in the cancer cell signify the transport of the Dendra2 labeled mitochondria in direct physical communication. All scale bars represent 10 μm length.

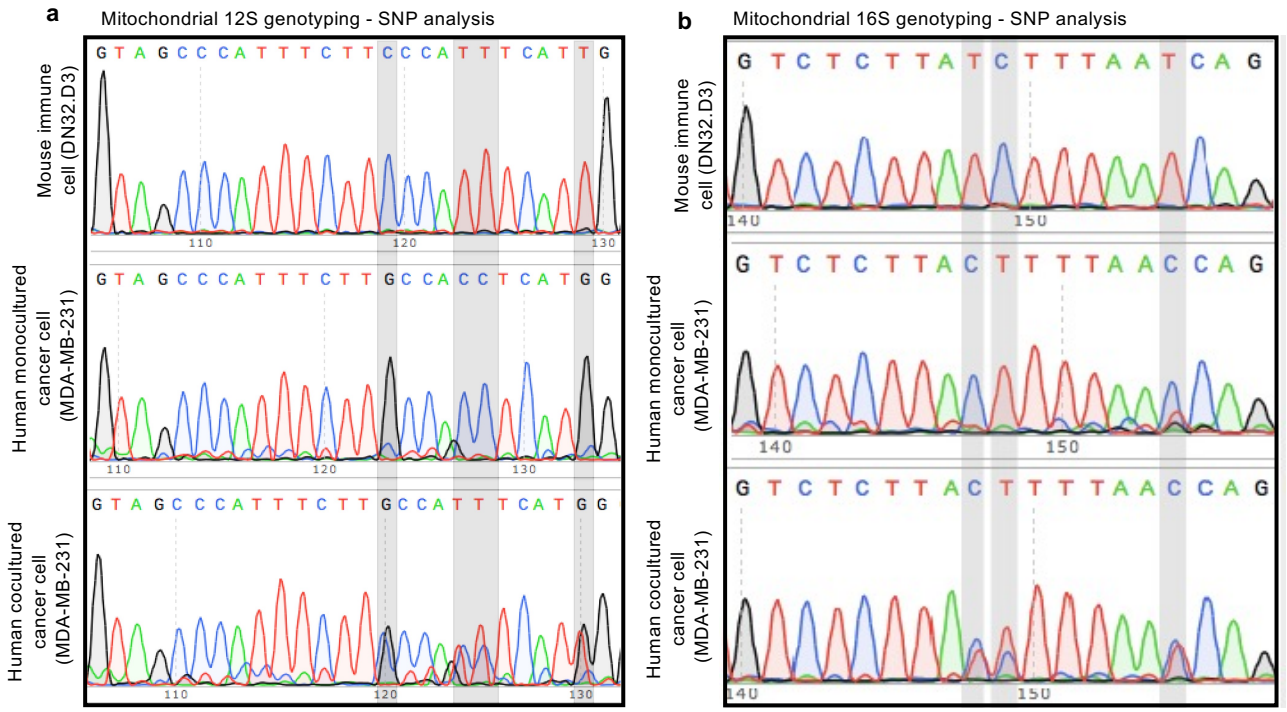

Supplementary Figure 12: Mitochondrial genotyping using species-specific single nucleotide polymorphisms (SNPs) to show mitochondrial acquisition from mouse NKT (DN32.D3) cells by human cancer (MDA-MB-231) cells. Forward and reverse primer pairs were constructed in conserved regions of both mouse and human mitochondrial (**a**) 12S and (**b**) 16S gene. Species-specific SNPs were identified for further analyses by comparing individual chromatograms and then compared with the cocultured cancer cells. Sequencing results confirmed predictions of SNPs in cocultured cancer cells, indicating that the cancer cell line MDA-MB-231 does show mitochondrial uptake from mouse NKT cell line DN32.D3. Single nucleotides (e.g. T or C) imply a homozygous genotype (i.e. TT or CC) at that position, whereas heterozygous genotypes (SNPs) are denoted as in column for cocultured cancer cells.

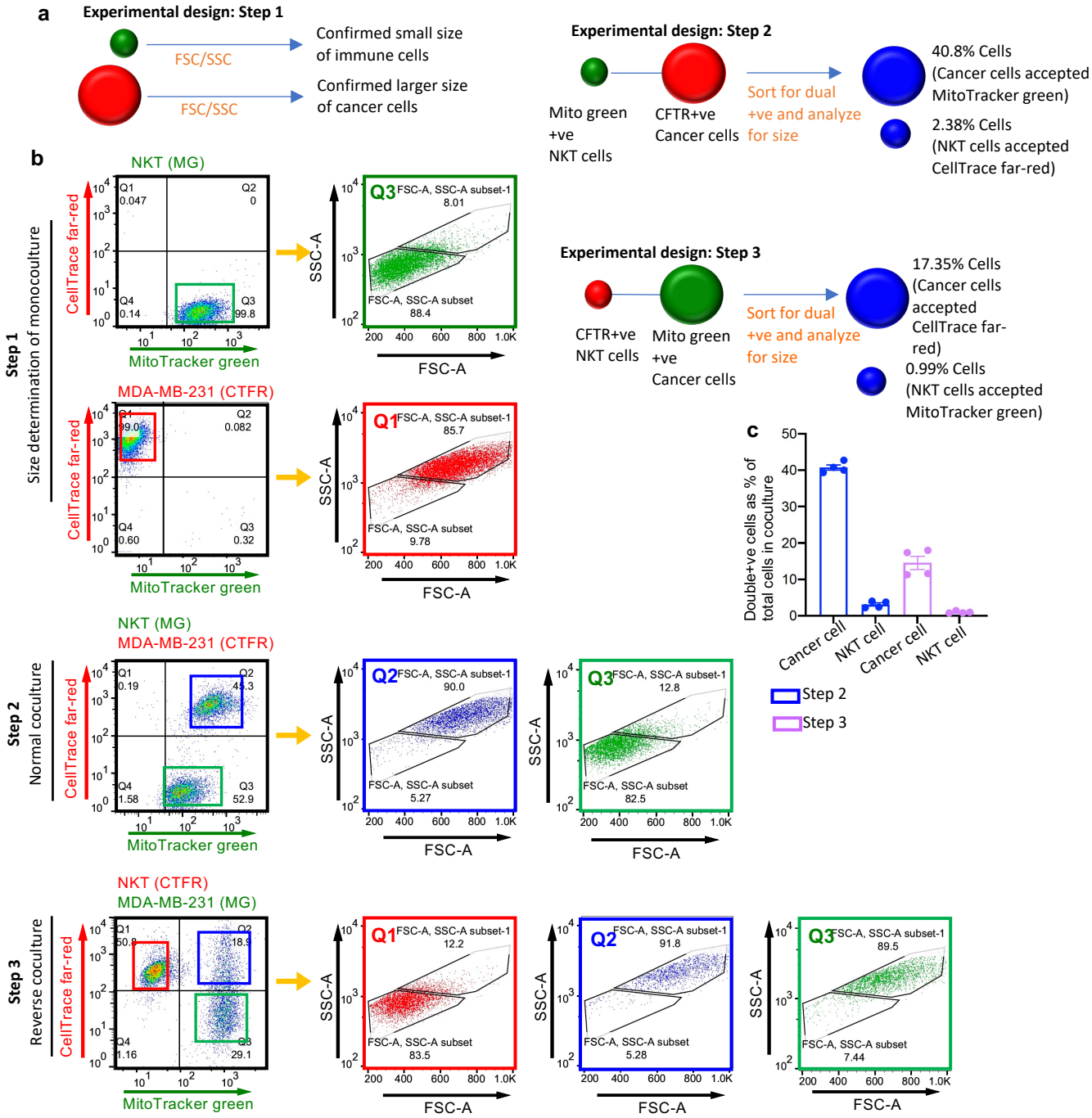

Supplementary Figure 13. Transfer of mitochondria is predominantly unidirectional from immune to cancer cells. (a) Schematic representation of experimental design and outcomes. (**b**) FACS plot based on size to demonstrate the preferential transport of the mitochondria from immune cells to cancer cells. The significant difference in the size of the cancer and immune cell makes it possible to distinguish the individual cell types based on the difference in forward scattering (FSC) and side scattering (SSC), i.e., cancer cells represents higher FSC and SSC values than that of immune cells (step 1). In step 2, the population exhibiting dual colors shows higher FSC and SSC value, which corresponds, to the population of the cancer (MDA-MB-231) cells. This indicates the cancer cells as the recipient cells of the labeled mitochondria and the immune cells are the donor. Similarly, for reverse coculture condition (step 3), i.e. NKT (CellTrace far-red) and MDA-MB-231 (MitoTracker green) coculture, again the population exhibiting dual colors exhibits higher FSC and SSC value corresponding to the cancer cell population. This indicates the cancer cells as the recipient cells of the cellular component and the immune cells are the donor. Although a negligible amount of transfer of cellular components from cancer cells to NKTs was observed in both cases, the dominant transfer of cellular organelles, such as mitochondria, is from immune to cancer cells. The similar gating strategy of Supplementary Fig 10d has been used to achieve the first scatter plot in each row. (**c**) Graph shows the transfer of mitochondria or cytoplasmic component to the recipient cell, i.e. dual +ve cells that emerges in the two experimental conditions.

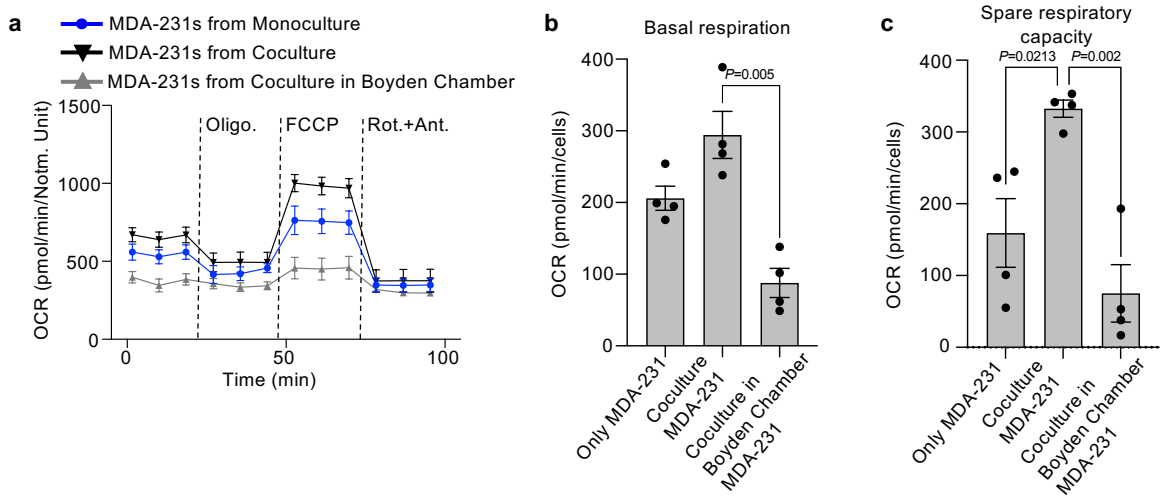

Supplementary Figure 14: Seahorse XF Mito-stress test profile shows augmented metabolism of cancer cells after coculture with CD3⁺ T cells, in terms of oxygen consumption rate (OCR), after coculture in comparison with the monocultured cells. Breast cancer cells (MDA-MB-231) were either grown in coculture with CD3⁺ T cells or separately as monocultures. CD3⁺ T cells and MDA-MB-231 cells were stained with CellTrace green and CallTrace far-red respectively and mixed to establish the coculture. After 16 h of coculture, the cells were separated by FACS and used for metabolism assay by Seahorse XF24. To obtain the oxygen consumption due to mitochondrial ATP production and maximal OCR, oligomycin (1 μM) and carbonilcyanide p-triflouromethoxyphenylhydrazone (FCCP) (1 μM) were added, respectively. Rotenone and antimycin-A were added (0.5 μM each) to block the mitochondrial activity. **(a)** The graph shows the increased mitochondrial respiration in cancer cells when they are cultured in presence of CD3⁺ T cells under conditions where nanotubes can form. The cancer cells obtained from coculture in presence of Boyden Chamber, where nanotubes can not form, show a lower mitochondrial respiration consistent with blockage of mitochondria transfer. Data represented as mean ± SEM (n = 4). (**b**-**c**) Graphs show basal respiration and spare respiratory capacity in cocultured and monocultured MDA-MB-231 cells. Data represented are mean ± SEM (n = 4, P = 0.0005 for basal respiration and P = 0.0213 and P = 0.002 for spare respiratory capacity). Statistical analysis was performed using one-way ANOVA with Tukey's multiple comparisons test.

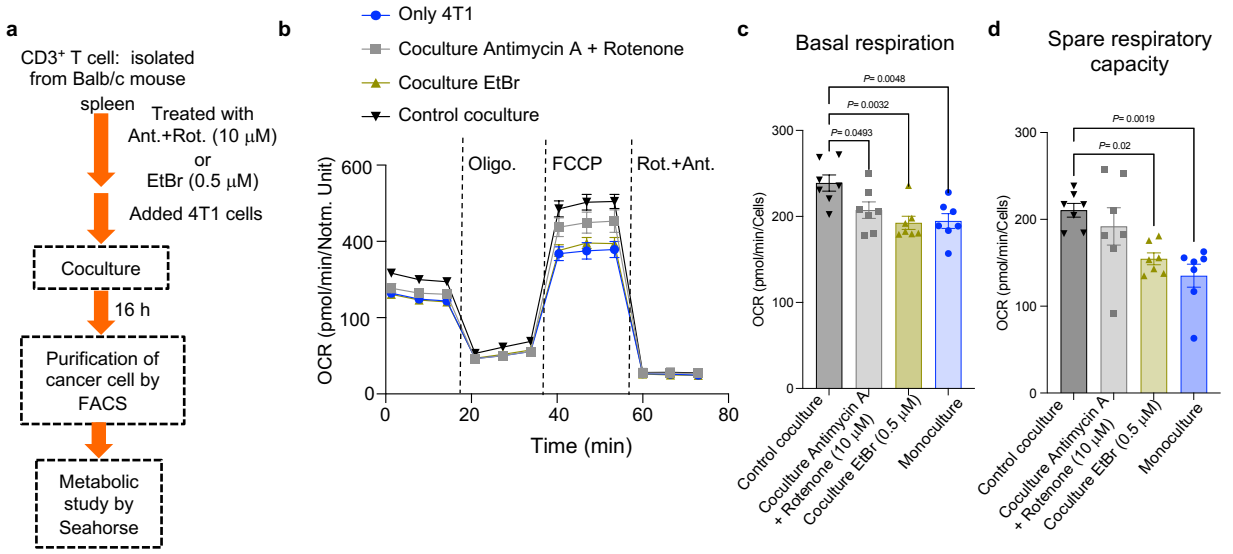

Supplementary Figure 15: Reduced augmentation of metabolism in cancer cells co-cultured with immune cell having dysfunctional mitochondria. (**a**) Schematic representation of the experimental design. CD3⁺ T cells were isolated from BALB/c mouse spleen and treated with either antimycin A + Rotenone (10 μM each) or EtBr (0.5 μM) for 1 h. The cells were washed and added to the coculture with 4T1 cells. After 16 h of coculture, the cells were separated by FACS and used for metabolism assay by Seahorse XF96. (**b**) Seahorse XF Mito-stress test profile shows difference in metabolism of cancer cells after coculture with healthy CD3⁺ T cells (control coculture, red line), with the immune cell having dysfunctional mitochondria (green and black line). To obtain the oxygen consumption due to mitochondrial ATP production and maximal OCR, oligomycin (1 μM) and carbonilcyanide p-triflouromethoxyphenylhydrazone (FCCP) (1 μM) were added, respectively. Rotenone and antimycin A were added (0.5 μM each) to block the mitochondrial activity. The graph shows the increased mitochondrial respiration in cancer cells when they are cultured in presence of CD3⁺ T cells under conditions where the cancer cell accept healthy mitochondria form immune cell. The cancer cells obtained from the treated coculture, where immune cell transfer dysfunctional mitochondria to cancer cell, show a lower mitochondrial respiration. Data represented are mean ± SEM (n = 6). (**c-d**) Graphs show basal respiration and spare respiratory capacity of 4T1 cells after cocultured with immune cell having healthy and dysfunctional mitochondria and monocultured 4T1 cells. Data represented are mean ± SEM (n = 6, $P < 0.01$ and $P = 0.05$). Statistical analysis was performed using one-way ANOVA with Dunnett's multiple comparisons test.

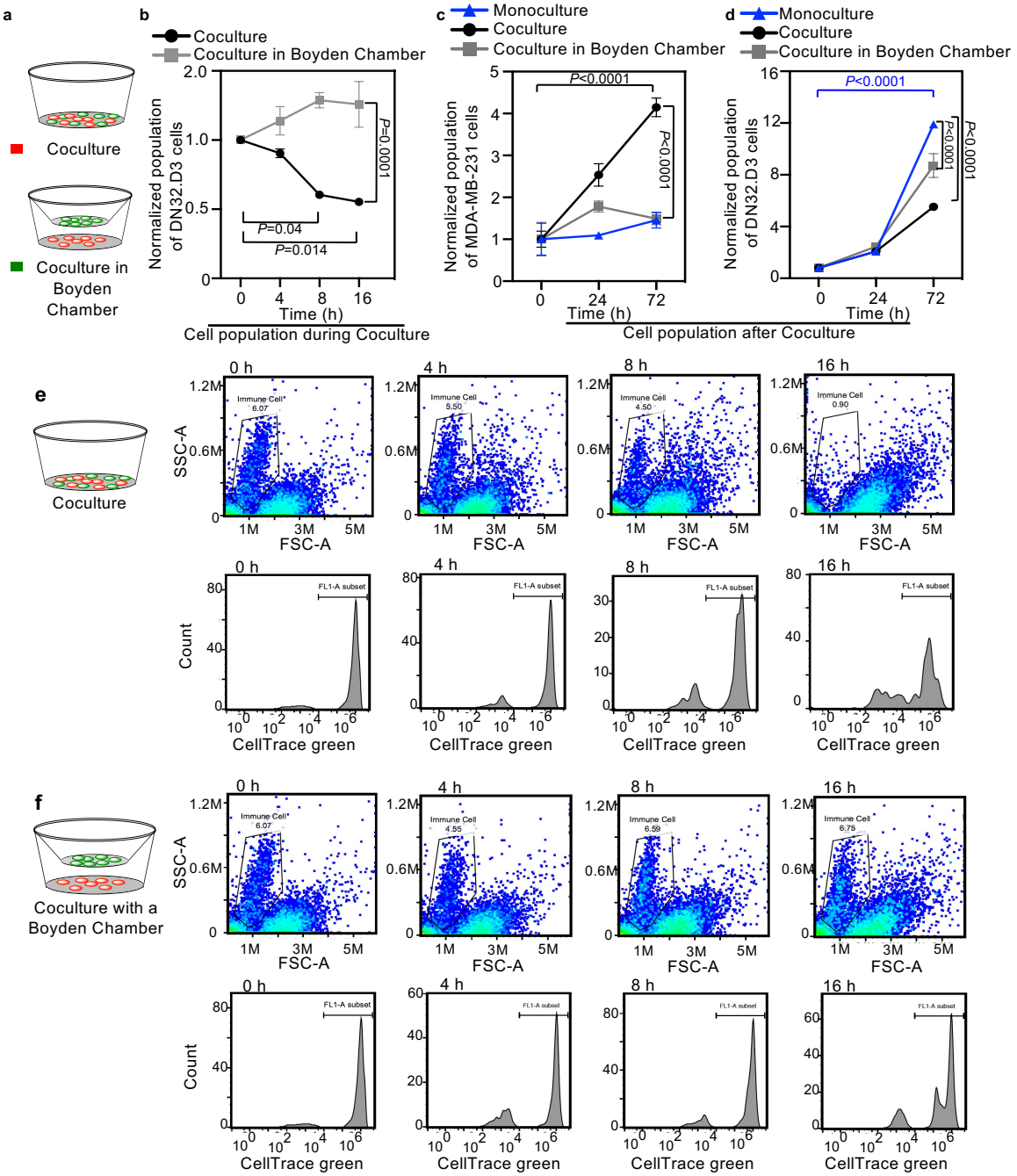

Supplementary Figure 16: Effect of metabolic gain or loss on immune and cancer cells viability. (**a**) Schematic representation of the experimental design. The immune cells (NKT) and cancer cells were cocultured in the same well, which allows nanotube formation, or separately in two chambers of a Boyden assay, which prevents physical nanotube connections. (**b**) Graph shows the time-dependent reduction of NKT cell population in coculture. The NKT cells populations in coculture were monitored by flow cytometry at different time points. All population data has been normalized with respect to the 0 h population and presented as the mean ± SEM of three independent experiments (n = 3). The graph shows a significant (P = 0.04 at 8 h and, P = 0.014 at 16 h) reduction in population of NKT cells in coculture but not in the Boyden assay. The population of the NKT cells in coculture at 16 h is significantly (P = 0.0001) reduced than that of coculture in Boyden chamber. Statistical analysis was performed using two-way ANOVA following Sidak's multiple comparison test. (**c**) Graph shows the proliferation of cancer cells and immune cells post coculture. The NKT and MDA-MB-231 cells were recovered after 16 h of coculture and, maintained further as monocultures for next 72 h. The data was normalized according to the population of 0 h for each cell and the data presented as mean ± SEM of three (n = 3) independent experiments. The graph shows significantly (P < 0.0001 for all) higher rate of proliferation of cancer cells isolated from the coculture, i.e., could gain mitochondria, compared with cancer cells from the Boyden assay or parent cancer cells that were maintained as monocultures to start with. Statistical analysis was performed using two-way ANOVA following Tukey's multiple comparison test. (**d**) Graph shows the reduction in rate of proliferation of cocultured NKT cells vs monocultured NKT cells at 72 h (n = 3, P < 0.0001 for all). Statistical analysis was performed using two-way ANOVA following Tukey's multiple comparison test. (**e**) Representative plots showing the change in population of immune cells (NKT) in coculture with cancer cells (MDA-MB-231). The coculture was analyzed by flow cytometry, and the population corresponding to the NKT cells (selected population in scatter plot) has been monitored at different time points. The data show significant reduction in NKT population with time. (**f**) Similar study in Boyden chamber shows a slight enhancement of NKT population with time.

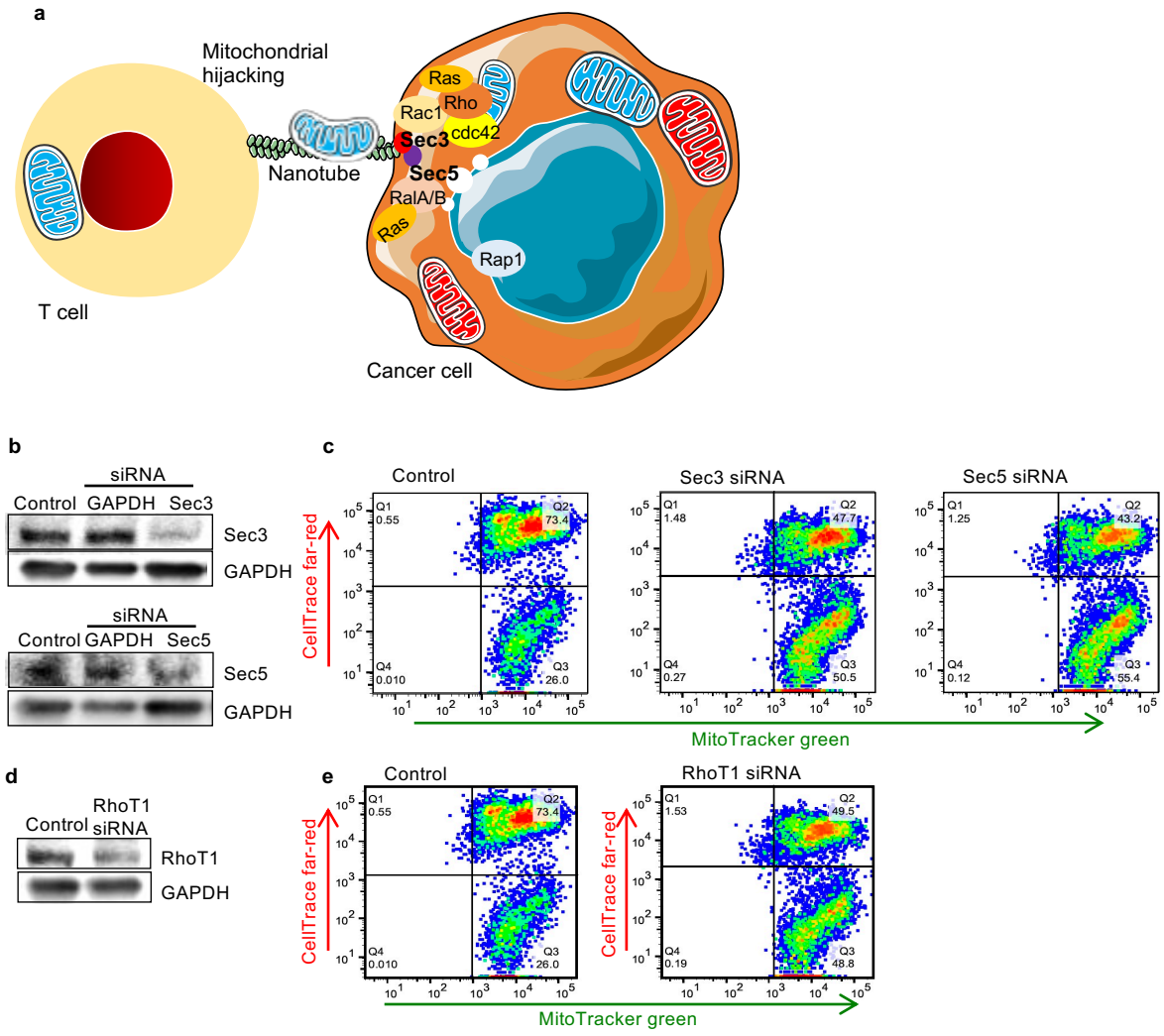

Supplementary Figure 17: Schematic shows the potential mechanism underlying nanotube formation and mitochondrial transfer. (**a**) The exocyst complex together with the Ras/Rho-GTPase family mediate actin remodeling for nanotube formation, and the Miro1-ATPase then facilitates mitochondria transfer over this bridge. (**b**) Immunoblot analysis to verify the knockdown of the Sec3 and Sec5. Cancer cells were transfected with either Sec3 or Sec5 siRNA (0.2 pM concentration) using Lipofectamine RNAiMAX according to the manufacturer's instructions. GAPDH siRNA was used as a control. (**c**) Scatter plot showing the transfer of mitochondria from NKT cells (DN32.D3) to cancer cells (MDA-MB-231) after knockdown of the Sec3 protein by transfection of Sec3 siRNA. The cancer and immune cells were stained with CellTrace far-red and MitoTracker green respectively and employed in coculture for 16 h. The flow cytometric analysis of the coculture after 16 h shows the significant reduction of the mitochondria transfer from immune to cancer cells. Transfer of mitochondria from NKT cells (DN32.D3) to cancer cells (MDA-MB-231) after knockdown of the Sec5 protein. The cancer and immune cells were stained with CellTrace far-red and MitoTracker green respectively and employed in coculture for 16 h. The flowcytometry analysis of the coculture after 16 h shows the significant reduction of the mitochondria transfer from immune to cancer cells. (**d**) Immunoblot analysis to verify the knockdown of the RhoT1. The immunoblot analysis signifies successful transfection and knockdown of the RhoT1 protein in cancer cell. GAPDH concentration did not change during the transfection process. (**e**) Scatter plot showing the transfer of mitochondria from immune cells (DN32.D3) to cancer cells (MDA-MB-231) after knockdown of the mitochondrial Rho-GTPase (RhoT1) by transfection of RhoT1 siRNA. The cancer cells were transfected by the RhoT1 siRNA for 12 h followed by culture in complete media for 48 h. The degree of knockdown was confirmed by immunoblot analysis. The cancer and immune cells were stained with CellTrace far-red and MitoTracker green respectively and employed in coculture for 16 h. The flow cytometric analysis of the coculture after 16 h shows the significant reduction of the mitochondria transfer from immune to cancer cells. The similar gating strategy of Supplementary Fig 10d has been used.

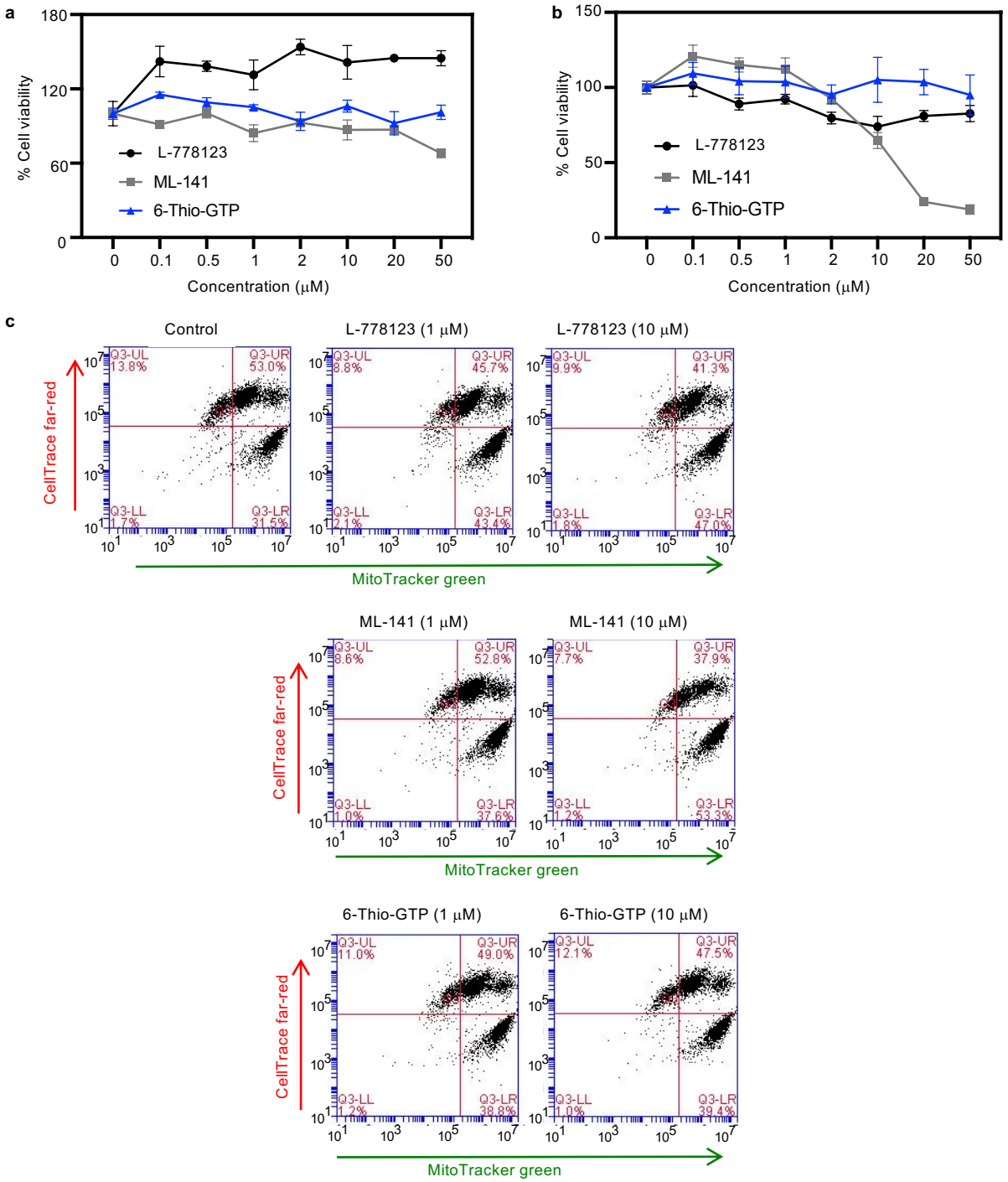

Supplementary Figure 18: Cell viability of (**a**) MDA-MB-231 and (**b**) 4T1 cells in presence of L-778123, ML-141 and 6-Thio-GTP. Different inhibitors were added to the respective cells in dose dependent manner and incubated for 7 h at basal media followed by incubation in complete media for 24 h. The cell viability was checked by MTT assay. No reduction in cell number was evident till 10 μM. Data presented mean ± SEM (n = 3). (**c**) The representative FACS plots show concentration-dependent reduction in mitochondria transport from immune to cancer cells in presence of the GTPase and GGTase inhibitors. MDA-MB-231 cells and NKT cells were treated with different concentration of inhibitor for 7 h and then added to establish the coculture assay. The NKT and cancer cells were stained with MitoTracker green and CellTrace far-red respectively, just before adding them into coculture. The transfer of mitochondria (upper right quadrant) was monitored by flow cytometry. Both ML-141 and L-778123 decrease the mitochondrial transfer in a concentration-dependent manner (data in upper right quadrant; the number decreases with increasing drug concentration). The similar gating strategy of Supplementary Fig 10d has been used.

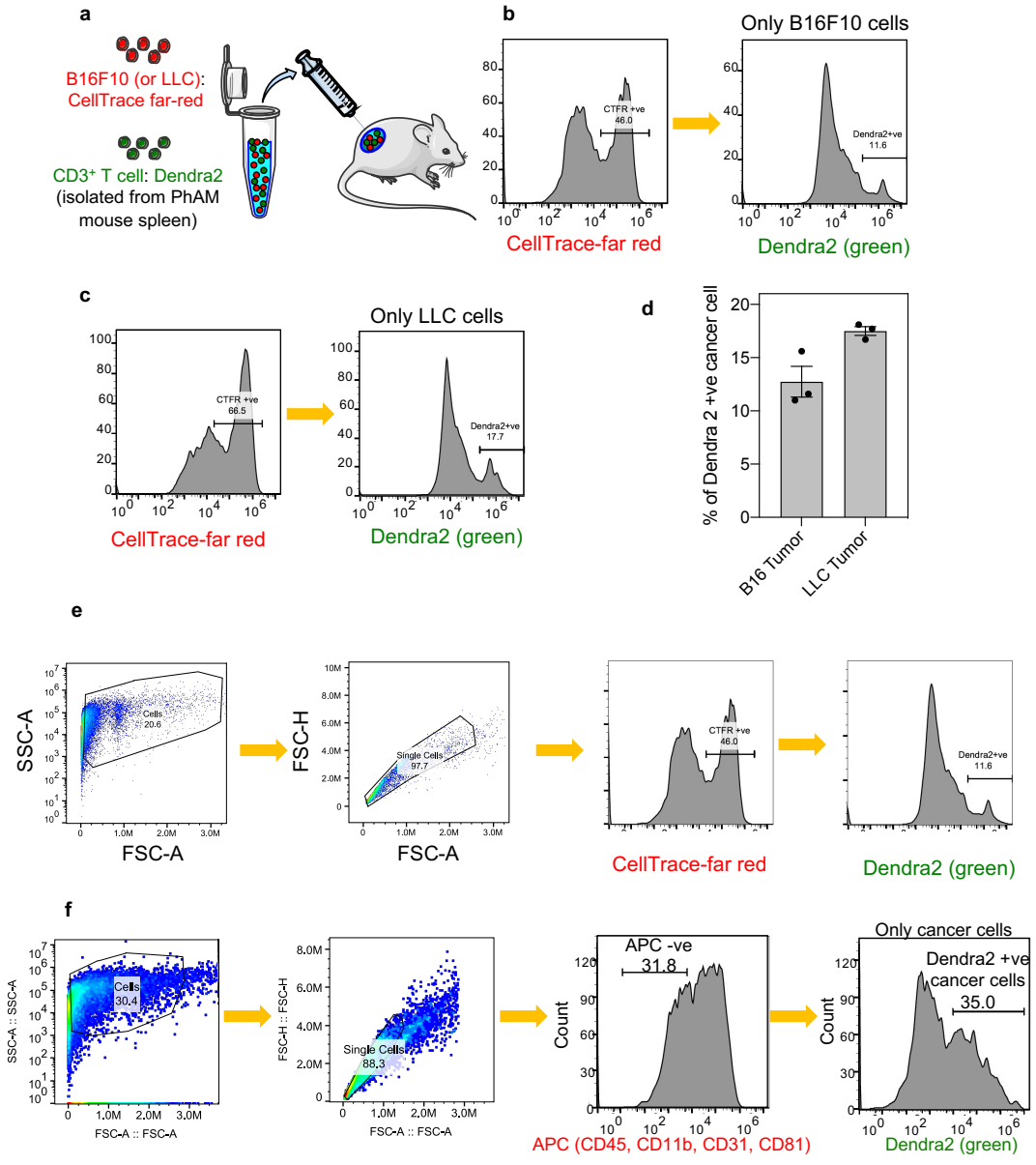

Supplementary Figure 19: The transfer of Dendra2-positive mitochondria from Dendra2-positive CD3⁺ T cells to B16F10 and LLC cells *in vivo*. (**a**) Schematic presentation of the experimental design for mitochondria transfer to B16F10 (or Lewis lung carcinoma, LLC) cells. Syngeneic B16F10 (or LLC) cells were labeled with CellTrace far-red and mixed with CD3⁺ T cells (Dendra2-positive, isolated from PhAM^{excised} mice spleen). The two cell types (1:1) were added in Matrigel (matrigel : PBS = 1 : 2) and injected subcutaneously in the right flank of PhAM^{excised} C57BL/6 mice. The matrigel plug was isolated from the mice after 60 h, and single cell suspension was prepared by collagenase digestion. The the lesser time point has been selected to avoid the involvement of infiltrating cells and loosing of CellTrace far-red intensity from cancer cells. (**b**) Histogram plot showing transfer of Dendra2-positive mitochondria in B16F10 cells. The cancer cells (B16F10) cells were selected by gating the CellTrace far-red high population and the amount of Dendra2+ve cells has been evaluated. Graph show 11.6% of cancer cells has been received mitochondria from Dendra2-positive CD3 T cells. (**c**) Histogram plot showing transfer of Dendra2-positive mitochondria in LLC cells. The cancer cells (LLC) cells were selected by gating the CellTrace far-red high population and the amount of Dendra2-positive cells has been evaluated. Graph show 17.7% of cancer cells has been received mitochondria from Dendra2-positive CD3⁺ T cell. (**d**) Bar plot showing the amount of cancer cells (CellTrace far-red +ve) accepted mitochondria (Dendra2-positive) from immune cell. Data shows mean ± SEM (n = 3). (**e**) Gating strategy for the flow-cytometric analysis. (**f**) Gating strategy of transfer of Dendra-2 labeled mitochondria to cancer cells in vivo. Lewis lung carcinoma cells were injected subcutaneously into syngeneic C57BL/6J PhAM^{excised} mice. Data presented in main figure 5a.

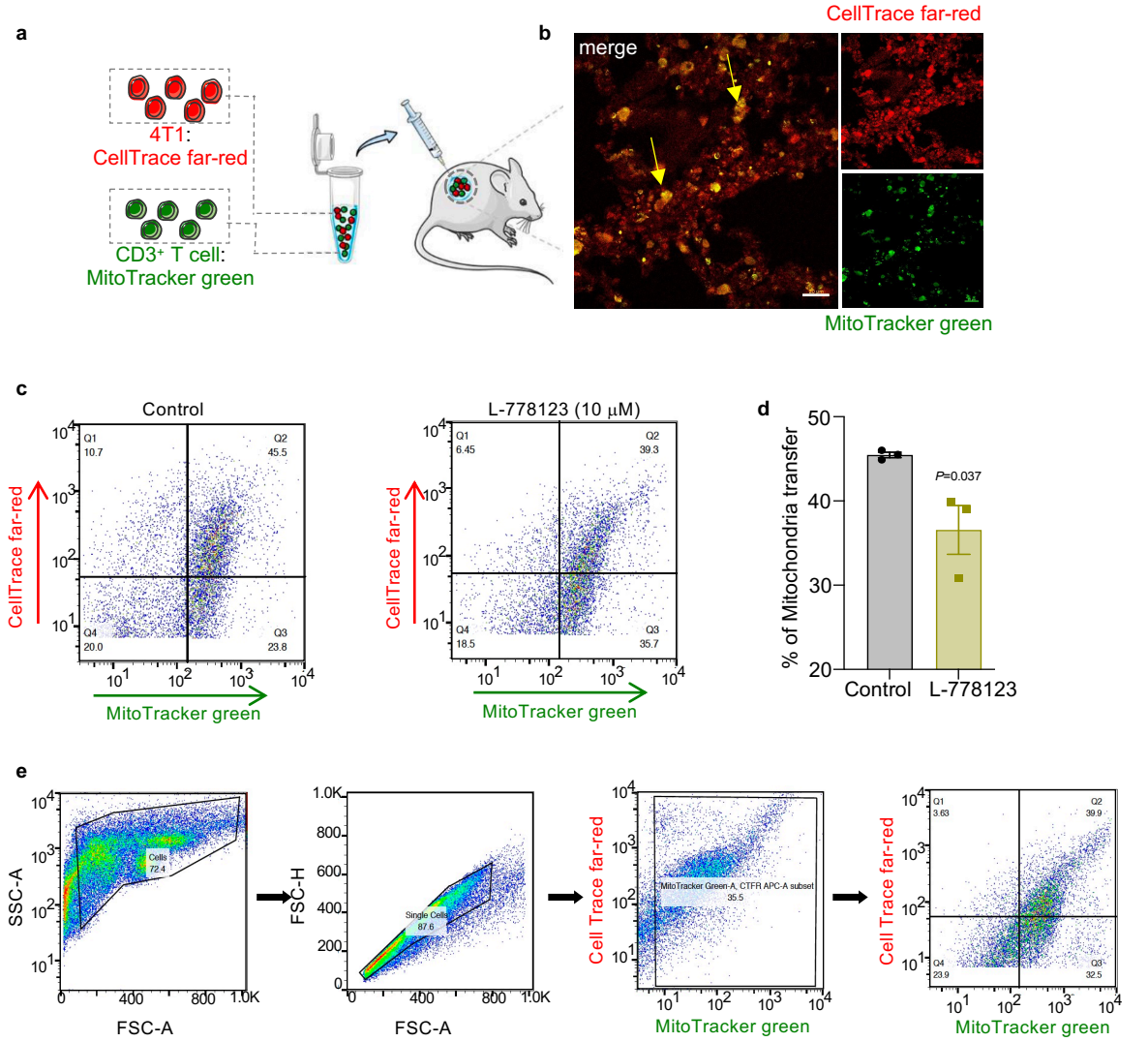

Supplementary Figure 20: Effect of pharmacological inhibition of nanotube on mitochondrial transfer, *in vivo*. (**a**) Schematic presentation of the experimental design for mitochondria transfer to 4T1 cells *in vivo*. Syngeneic 4T1 cells were labeled with CellTrace far-red and mixed with MitroTracker green stained CD3+ T cells. The two cell types (1:1) were added in Matrigel (matrigel : PBS = 1 : 2) and injected subcutaneously in the right flank of BALB/c mice. (**b**) Confocal image shows the transfer of mitochondria from CD3+ T cells to 4T1 cells *in vivo* (scale bar = 20 μm). Syngeneic CD3+ T cells and 4T1 cells were labeled with MitoTracker green and CellTrace far-red, respectively. The two cell types were added (1:1) in Matrigel (matrigel : PBS = 1 : 2), and injected subcutaneously in the right flank of BALB/c mice. The matrigel plug was isolated from the mice after 24 h, and thin tissue slices (20 μm) were prepared. Confocal image shows significantly higher number of cancer cells (red) as opposed to immune cells (green) in the plug. A subset of cells appear yellow in the merge image, consistent with MitoTracker-labeled mitochondria in the cancer cells, signifying mitochondrial transfer from the T cells to the cancer cells. Note that the directionality of transfer, established earlier, is from immune cells to cancer cells. (**c**) Graph shows mitochondrial transfer from immune cells to cancer cells *in vivo* experimental set up, as analyzed by flow cytometer. The matrigel plug was isolated from the mice after 24 h, and single cell suspension was prepared. The scatter plot represents the transfer of mitochondria to cancer cells (upper right quadrant) from the immune cells, and the inhibition of mitochondrial transfer in the presence of the inhibitor (L-778123). (**d**) Representative bar graph shows mitochondrial transfer from immune cells to cancer cells in the above in vivo experimental set up, as analyzed by flow cytometer. Treatment with L-778123 (10 μM) to block nanotube assembly reduces the mitochondria transfer. Data shown are mean ± SEM (n = 3, *P* = 0.037). Statistical analysis was performed using unpaired t-test, two-tailed. The matrigel plug was isolated after 24 h and single cell suspension has been prepared. The transfer of mitochondria from CD3+ T cells to 4T1 cells was analyzed by flow cytometer and the amount of cancer cell having both red and green fluorescence has been evaluated. (**e**) Gating strategy for matrigel experiment. Only the red and green positive populations have been considered because a large number of infiltrated cells disturbs the consistency of the data.

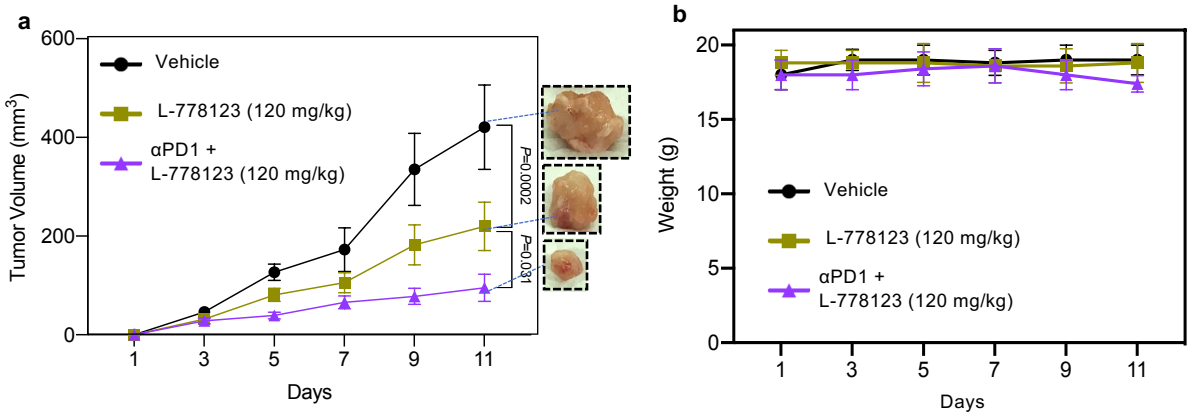

Supplementary Figure 21: (**a**) Tumor growth curves and representative image of the tumors show the effect of L-778123 and PD1 immune checkpoint inhibitor (ICI). Syngeneic immunocompetent BALB/c female mice were injected with 4T1 cells and treated with 6 cycles of inhibitors administered intraperitoneally. Data shown are mean ± SEM (n = 5 per group). Treatment with L-778123 (120 mg/kg) significantly inhibited tumor progression (P = 0.002). Statistical analysis was performed using two-way ANOVA with Tukey's multiple comparisons test. The combination of PD1 + L-778123 (120 mg/kg) significantly improved antitumor response vs vehicle (P < 0.001). (**b**) Effect of different treatments on the body weight. Change in body weight was monitored as a measure of gross toxicity. The different treatments are labeled above. The first drug injection was made on the day 1 and subsequent injections were made in every alternate day for 6 cycles. Data is presented as mean ± SEM (n=5). No significant weight loss was seen at the doses used.

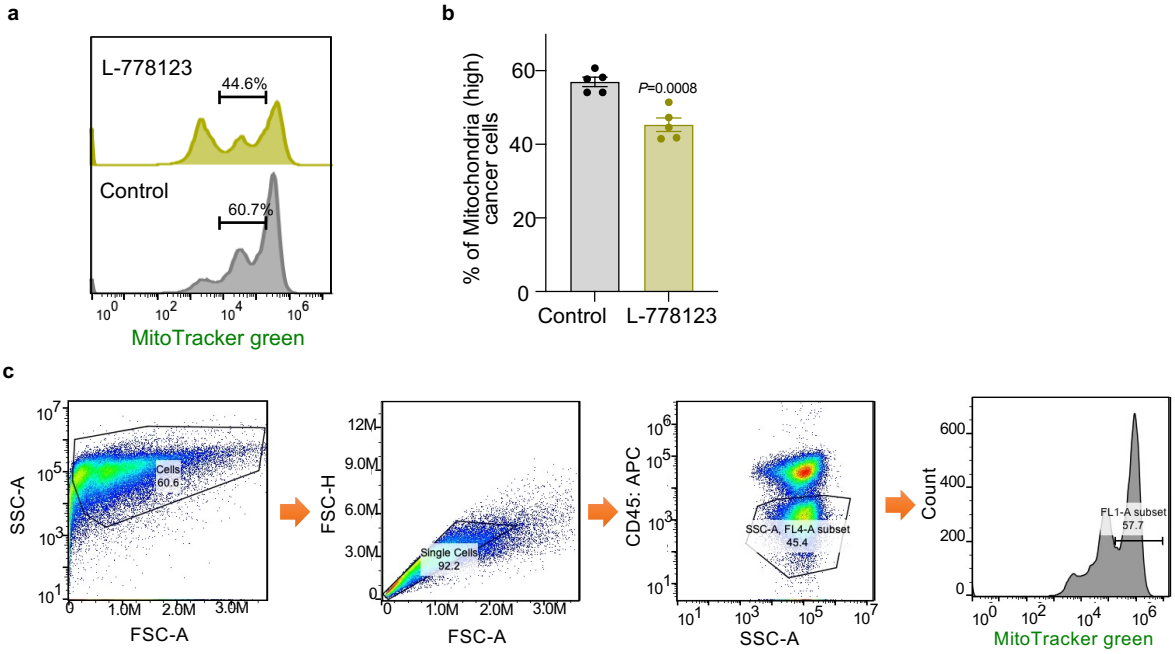

Supplementary Figure 22: Treatment with L-778123 blocks mitochondrial gain in cancer cells, in vivo. (**a**) Histogram plot showing the distribution of mitochondria in cancer cells in control and L-778123 treated condition. Syngeneic immunocompetent BALB/c female mice were injected with 4T1 cells and treated with 6 cycles of inhibitors administered intraperitoneally. The tumors were isolated after 6 cycle of injection and the single cell suspension was prepared by collagenase digestion. The cell suspension was stained with MitoTracker green followed by CD45 (APC) antibody. The MitoTracker intensity of CD45 –ve population i.e, the majority of cancer cell, has been monitored and plotted in the histogram. The population of cancer cells representing highest intensity of the MitoTracker green were considered as the cancer cell, which has accepted excess mitochondria from neighboring cells. The population of the cancer cells with highest MitoTracker intensity was found to reduce in case L-778123 treated group with a simultaneous new population with low mito-intensity has appeared. (**b**) Bar diagram showing reduction of mitochondria transfer by L-778123. The population of cancer cells representing highest intensity of the MitoTracker green has been monitored in case of control and L-778123 treated group. A significant reduction of the cancer cell population, having high number of mitochondria, has been observed in case of L-778123 treated group. Data represented as mean ± SEM. (n = 5 per group, *P* = 0.0008). Statistical analysis was performed using unpaired *t*-test, two-tailed. This observation confirms the reduction of mitochondria transfer by L-778123. (**c**) Gating strategy for the flow cytometer experiment to study the level of mitochondria in cancer cells in control and L-778123 treated condition. The mitotracker intensity of CD45 –ve population has been monitored and plotted in the histogram. The population of cancer cells representing highest intensity of the MitoTracker green corresponds to the cancer cells which have accepted excess mitochondria from neighboring cells. The population of cells with highest MitoTracker intensity was found to reduce in case L-778123 treated group with a simultaneous new population with low mito-intensity. This observation confirms the reduction of mitochondria transfer by L-778123.

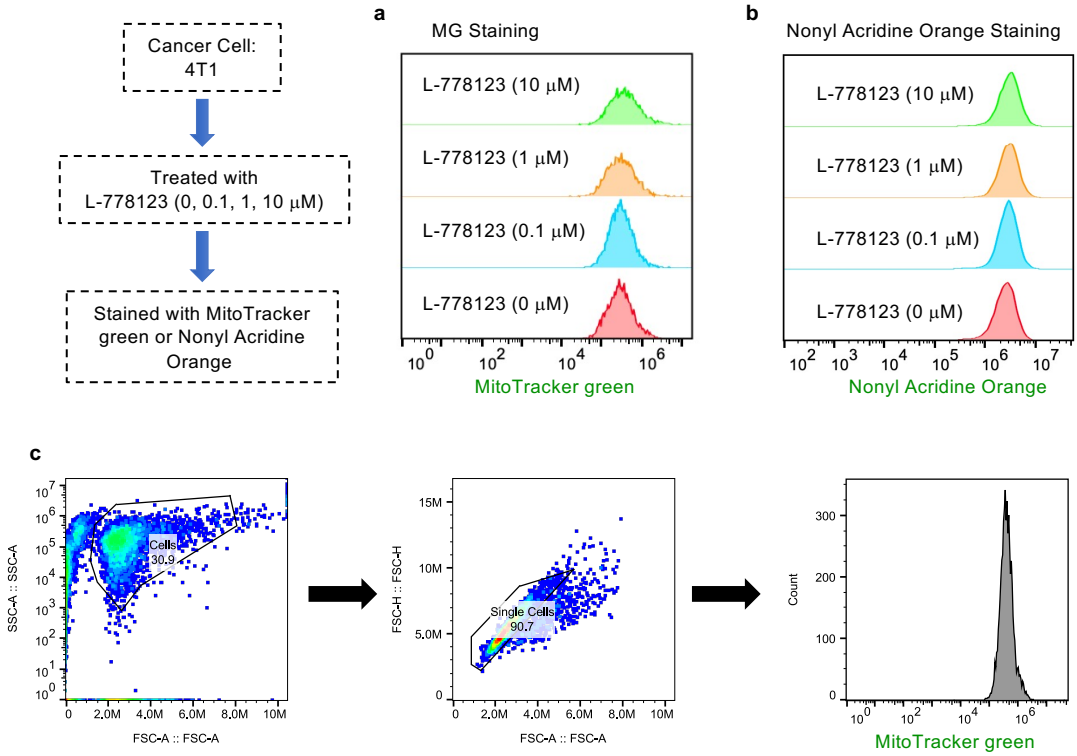

Supplementary Figure 23: L-778123 treatment has no effect on mitochondrial mass of cancer (4T1) cell. The histogram plot showing no change in the mitochondrial mass of 4T1 cells upon treatment with L-778123. 4T1 cell were treated with different concentration of L-778123 for 7 h in basal media followed by 16 h in complete media. The cells were washed and stained separately with MitoTracker green (**a**) and nonyl acridine orange (**b**) and analyzed by flow cytometer. No change in the MitoTracker green and nonyl acridine orange intensity has been observed, which represents to the equal mitochondrial mass upon L-778123 treatment on cancer cell. (**c**) Gating strategy for the flow-cytometric analysis.

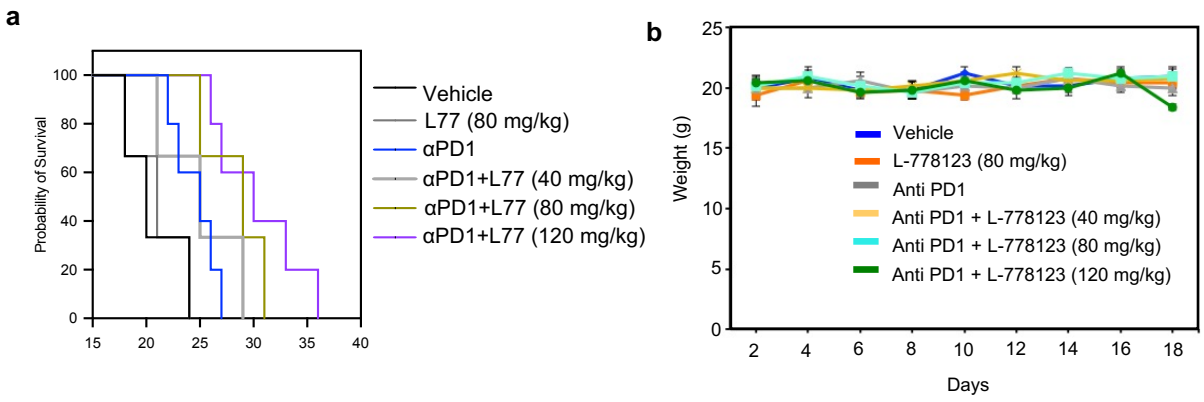

Supplementary Figure 24: Combination of immune checkpoint inhibitors and pharmacological inhibitor of nanotubes increases survival in breast cancer model, in vivo. (**a**) Kaplan Meier survival curve for the different treatment groups. The combinations show a dose-dependent improvement in survival (n = 5 per group, *P* = 0.0006 vs vehicle control). (**b**) Effect of different treatments on the body weight. Change in body weight was monitored as a measure of gross toxicity. The different treatments are labeled above. The first drug injection was made on the day 2 and subsequent injections were made in every alternate day for 8 cycles. Each group contains 5 animals (n = 5) and the data is presented in mean ± SEM. No weight loss was seen at the doses used.

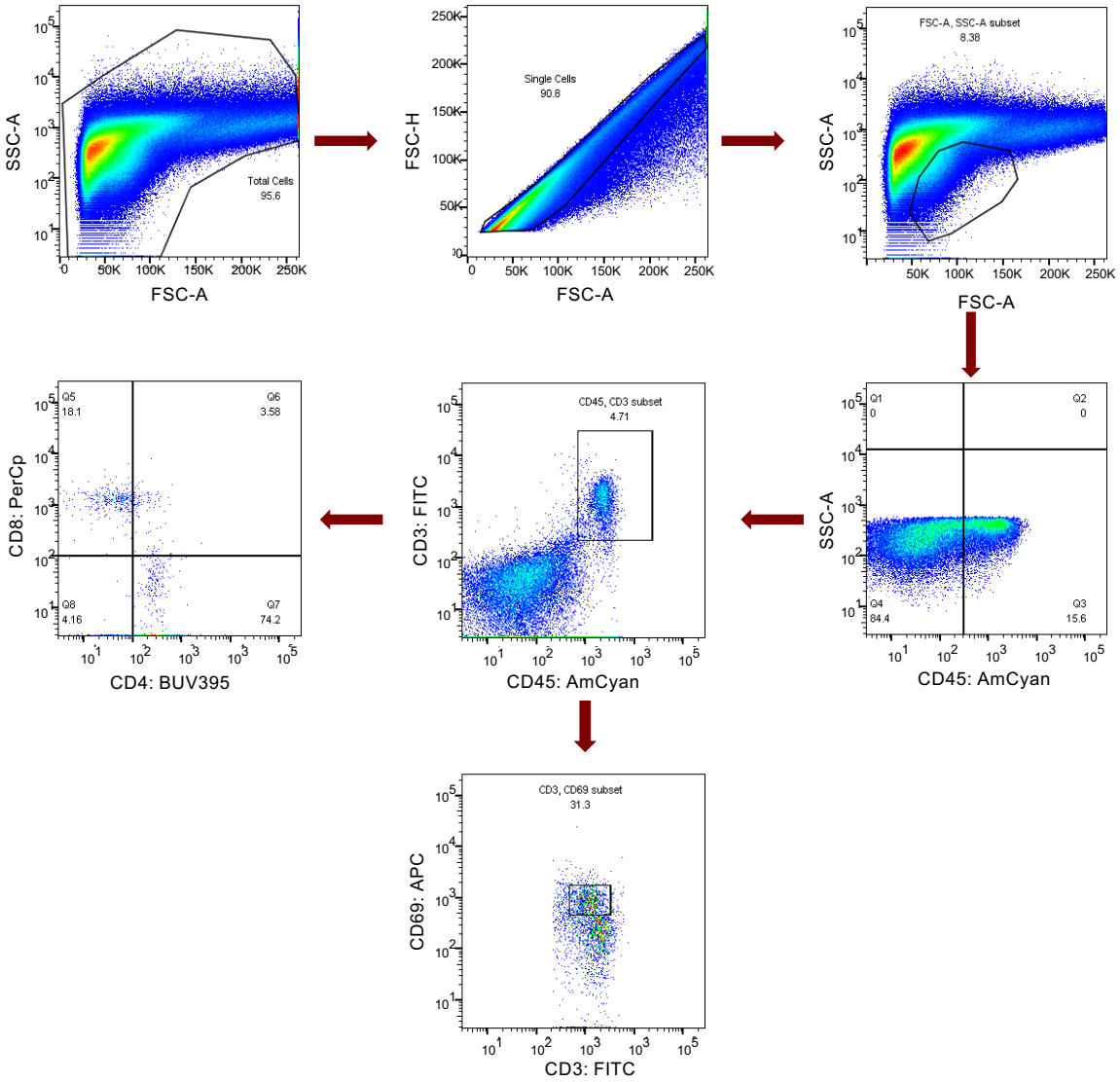

Supplementary Figure 25: Gating strategy for flow cytometry analysis of the single cell suspension of mice tumors. The tumors were isolated from mice after 8 injection cycle, and single cell suspension was prepared. The cell suspension were stained with series of fluorophore-conjugated antibodies and analyzed through flow cytometry. The figure shows the strategy of stepwise gating for flow cytometric analysis.

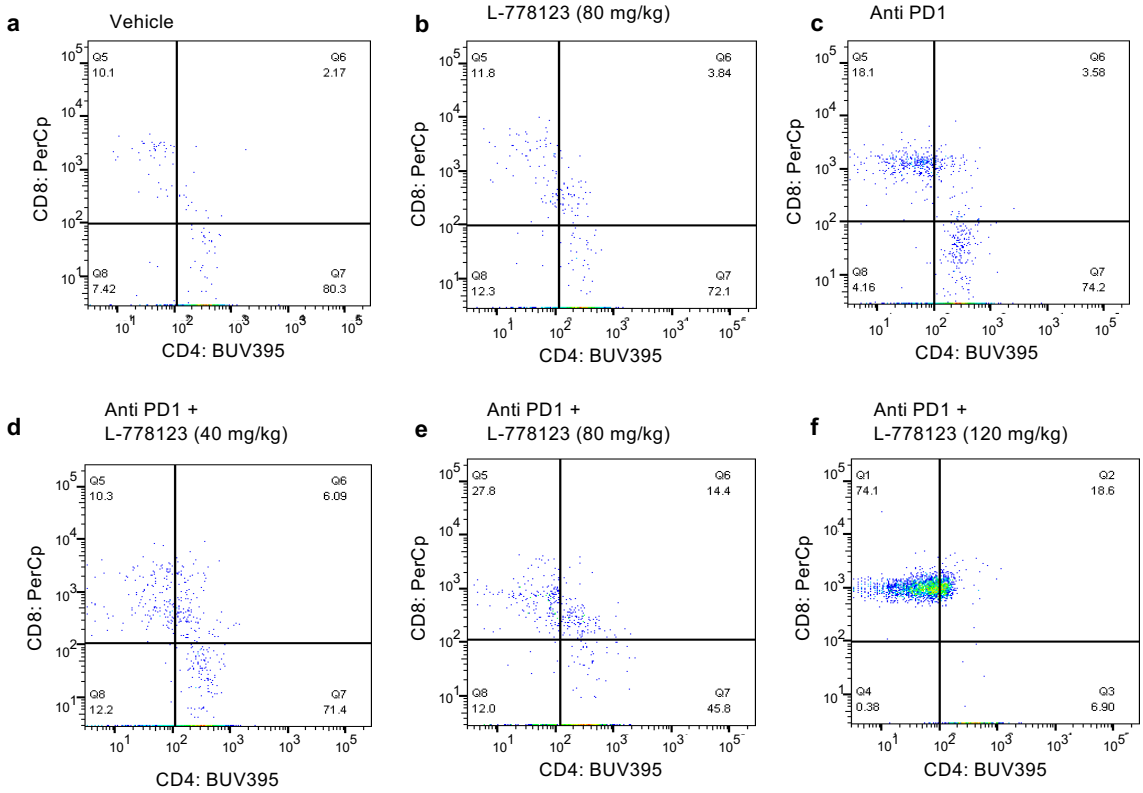

Supplementary Figure 26: Flow cytometric analysis of the CD8⁺ T cell population in the tumor cell suspension obtained from mice. The tumors were isolated from mice after 8 injection cycle and single cell suspension was prepared. The cell suspension were stained with series of fluorophore-conjugated antibodies and analyzed through flow cytometry. The representative plots show the change in population of cytotoxic T cell (CD8⁺ T cell) between each treatment group. A significant enhancement of CD8⁺ T cell population was observed in case of drug treated groups.

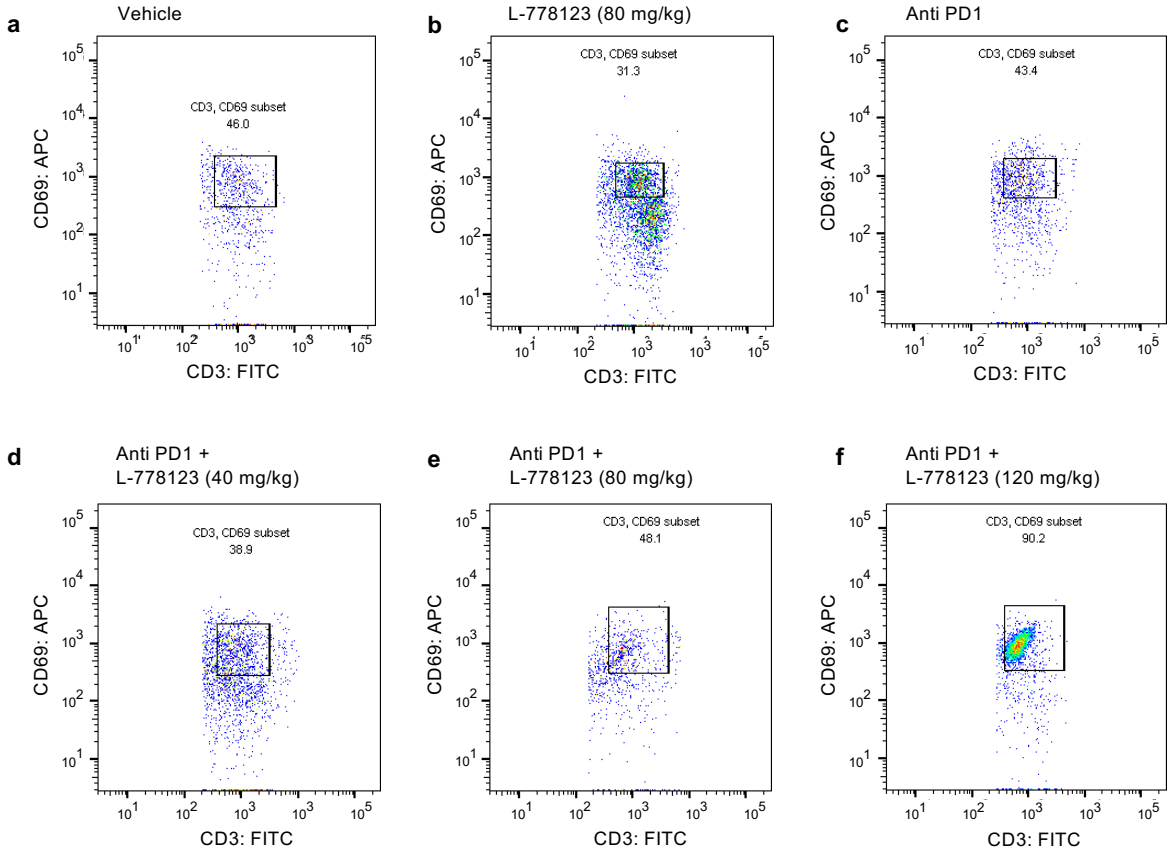

Supplementary Figure 27: Flow cytometric analysis of the activated T cell population ($CD69^+$) in the tumor cell suspension obtained from mice. The tumors were isolated from mice after 8 injection cycle, and single cell suspension was prepared. The cell suspension were stained with series of fluorophore-conjugated antibodies and analyzed through flow cytometry. The representative plots show the change in population of activated T cell ($CD69^+$) between each treatment group. A significant enhancement of activated T cell population was observed in case of drug treated groups.

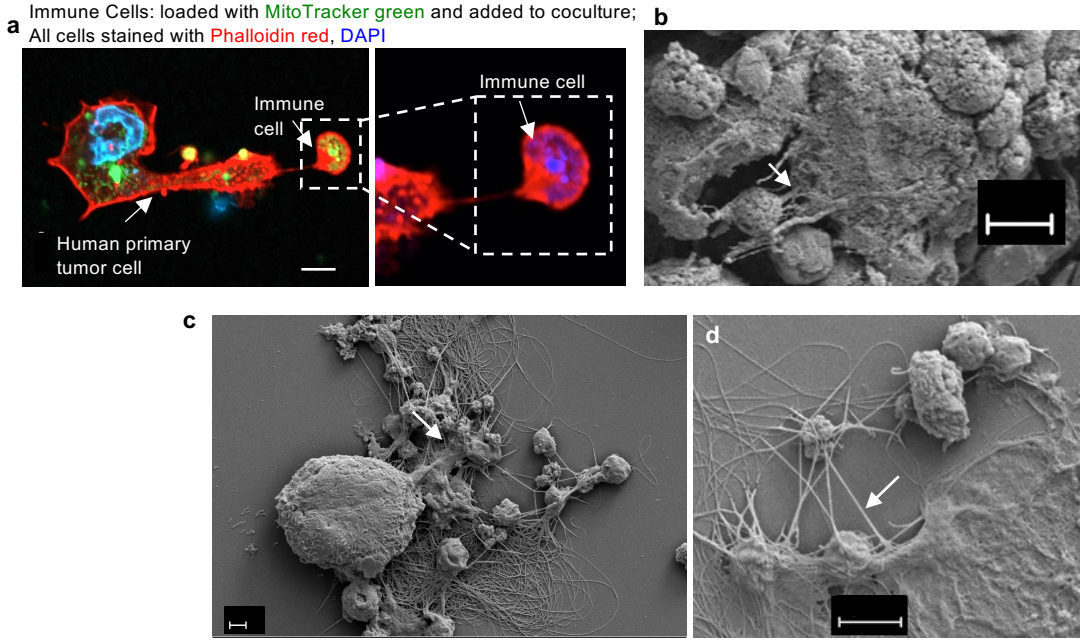

Supplementary Figure 28: (**a**) Confocal imaging shows that nanotube formation and mitochondrial transfer occurs in clinically-isolated samples. Human PBMCs were stained with MitoTracker green and cocultured with a primary human cancer explant (scale bar = 5 μm). The actin and nucleus were stained with phalloidin red and DAPI, respectively. The nucleus staining in the immune cell not visible because of the masking of the blue intensity by highly intensed cancer cell mitochondria. (**b-d**) Representative FESEM image shows nanotube formation between primary human tumor cell explants and an autologous immune cells. Explants generated from primary human tumor biopsy from three independent donors ((**b**) thymoma, (**c-d**) metastatic breast cancer in liver and metastatic breast cancer to peritoneum) were cultured with PBMCs obtained from the matched patient's blood (scale bar c = 1 μm, d = 2 μm). The explant-immune cell cocultures was fixed at 16 h post-coculture and imaged using FESEM. This data represents the formation of nanotube between cancer cells and immune cells in human clinical samples.

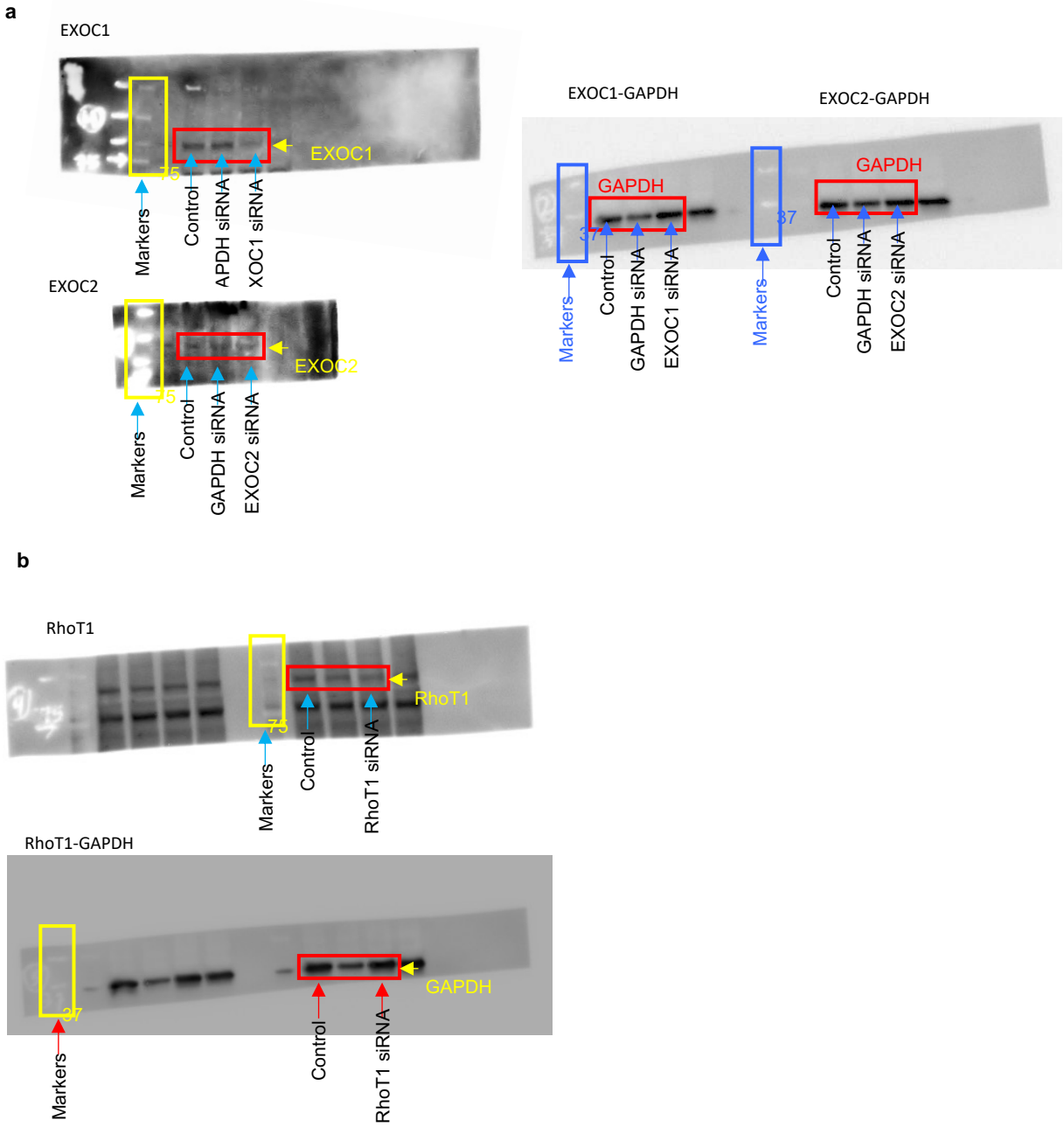

Supplementary Figure 29: (**a**) Complete uncropped western blot data of supplementary figure 17b. (**b**) Complete uncropped western blot data of supplementary figure 17d.

Supplementary Table 1: Mitochondrial genotyping using species (and cell line) specific single nucleotide polymorphisms (SNPs) to show mitochondrial acquisition from mouse NKT cell line DN32.D3 into human cancer cell line MDA-MB-231.

Mitochondrial Gene (also known as)	**Primers used for amplification and sequencing**	**Expected product length (bp)**		**SNPs**	**Mouse NKT cell line DN32.D3**	**Human cancer cell line MDA-MB-231**	**Cocultured cancer cells**
		Mouse DN32.D3	**Human MDA-MB-231**		**Genotype (position)**	**Genotype**	**Genotype**
16S (MT-RNR2)	F1 (ACCCCGCCTGTTTACCAAAAACATC) R1 (AAGCTCCATAGGGTCTTCTCGTCTT)	313 bp	253 bp	1	T (148 bp)	C	T/C
				2	C (149 bp)	T	T/C
				3	T (171bp)	G	T/G
				4	T (172 bp)	C	T/C
				5	A (174 bp)	C	A/C
	F2 (CCTAGGGATAACAGCGCAATCCTAT) R2 (TATTTCTCTTGTCCTTTCGTAC)	217 bp	218 bp	1	T (148 bp)	C	T/C
				2	C (149 bp)	T	C/T
				3	T (155 bp)	C	T/C
12S (MT-RNR1)	F1 (AGCTAAGACCCAAACTGGGATTAGA) R1 (AGGGTTTGCTGAAGATGGCGGTATA)	231 bp	226 bp	1	T (140 bp)	C	T/C
				2	A (152 bp)	G	A/G
	F2 (ACGTTAGGTCAAGGTGTAGCC) R2 (TTGAGGAGGGTGACGGGCGGTGTGT)	182 bp	182 bp	1	A (70bp)	T	A/T
				2	T (79 bp)	C	T/C
				3	A (98 bp)	T	A/T